Sensors & Diagnostics

CRITICAL REVIEW

View Article Online
View Journal | View Issue

Cite this: *Sens. Diagn.*, 2024, **3**, 946

Recent developments in pyrene-based fluorescence recognition and imaging of Ag^{+} and Pb^{2+} ions: Synthesis, applications and challenges

Suvendu Paul, *[a] Prasenjit Barman, [b] Nilanjan Dey [a] and Michael Watkinson *[cd]

Contamination of heavy metals in the environment is a burning and contemporary issue of modern life. Whilst lead contamination is historic, the ongoing extensive use of lead in batteries is likely to continue to cause serious environmental problems. Silver ions also present multiple environmental issues, such as bioaccumulation and toxicity. As a result, these two heavy metal ions have a high impact from an environmental and industrial point of view. Thus, the colorimetric and fluorescence detection of these two metal ions has been the subject of intense research during the last decade and pyrene-based fluorophores have played a crucial role in their detection. This review article summarizes the recent chronological progress on pyrene moiety integrated small molecule chemosensors for the colorimetric and fluorescent detection of silver and lead ions. Herein, the different strategies that have been utilized for the recognition of lead and silver ions are discussed. Throughout, the juxtaposition of structural aspects of the chemosensors and their sensitivity has been scrutinized together with an overview and future vision.

Received 27th October 2023,
Accepted 22nd April 2024

DOI: 10.1039/d3sd00289f

rsc.li/sensors

[a] *Department of Chemistry, BITS-Pilani, Hyderabad Campus, Hyderabad, Telangana-500078, India. E-mail: paul.suvendu2016@gmail.com*
[b] *Department of Chemistry, Kaliyaganj College, West Bengal-733129, India*
[c] *The Lennard-Jones Laboratories, School of Chemical and Physical Science, Keele University, ST5 5BG, UK*
[d] *Department of Natural Sciences, Faculty of Science and Engineering, Manchester Metropolitan University, Chester Street, Manchester, M1 5GD, UK. E-mail: m.watkinson@mmu.ac.uk*

Introduction

The colorimetric and fluorescence detection of different kinds of analytes has become a convenient tool of the modern era for several reasons, including high selectivity and sensitivity, the naked-eye colour change phenomenon, low technical need and

Suvendu Paul

Suvendu Paul was born in West Bengal, India. He obtained his B. Sc. and M.Sc. with a major in Chemistry from The University of Burdwan, West Bengal, India. Thereafter, he completed his doctoral research under the joint supervision of Dr. Tapas Majumdar and Dr. Arabinda Mallick from the University of Kalyani. His research covers the synthesis of small organic fluorophores and colorimetric and fluorescence detection of anions, cations, ion-pairs, small biological molecules and explosive molecules. He is also interested in the photophysical study of different bioactive fluorophores in homogeneous and micro-heterogeneous liquid environments like aqueous cyclodextrin, micelles, reverse micelles and serum albumin proteins using spectroscopy, molecular docking and DFT calculations.

Prasenjit Barman

Prasenjit Barman was born in West Bengal, India. He received his undergraduate degree in Chemistry from The University of Burdwan, West Bengal, India and his Master's degree in Chemistry from the Indian Institute of Technology (IIT), Guwahati, India. In 2016, he earned his Ph.D. in Chemistry from the IIT, Guwahati under the mentorship of Prof. Chivukula V. Sastri. He was a postdoctoral associate with Prof. Stuart James and a Newton International Post Doctoral Fellow at The Queen's University Belfast, United Kingdom (UK). He was involved there in understanding the kinetics of mechanochemical reactions. Later in 2020, he joined as an Assistant Professor at the Department of Chemistry, Kaliyaganj College. Since then, his main research interests have been in solid-state chemistry, green chemistry and materials synthesis.

expense, rapid response, low toxicity, and *in vivo* and *in vitro* compatibility.[1–6] As a result, these strategies have now been widely employed in the detection of a broad range of important analytes in biology, physiology, medicine, pharmacology and environmental sciences.[1] In recent years, pyrene-based optical probes have received enormous attention due to their efficacy in a wide range of applications, including fluorescence studies,[7–9] environmental monitoring,[10] bioimaging[11] and organic electronics.[12,13] In solution, pyrene can exist both in monomer and excimer forms.[14,15] Excimers have distinct spectroscopic properties compared to individual pyrene molecules, including a redshift in emission wavelength, and altered fluorescence lifetimes.[15] The excimer formation is sensitive to environmental factors such as temperature and viscosity,[16] pressure,[17] pH,[18] and molecular confinement, making it useful in the study of local microenvironments.[10] Upon light absorption, pyrene can populate both singlet and triplet excited states. The intersystem crossing from the singlet to the triplet state is relatively efficient, and the triplet state is involved in some photochemical reactions, including sensitized photooxidation.[14,15] This is particularly important to detect oxygen concentrations and monitor oxidative processes.

Though fluorescent chemosensors might be composed of various signalling moieties like BODIPY, indolylmethanes, carbohydrate-derived macrocyclic compounds, coumarin, cyanine, cucurbituril, naphthalene diimides, nitrobenzoxadiazole, calix[4]arene, calixarenes, pillar[*n*]arene, DNA-based sensors, porphyrins, *etc.*, pyrene holds some additional advantages, particularly in the context of fluorescence imaging. Basically, pyrene units are involved in aggregation. Within different micro-environments such as encapsulation within protein entities, surfactants, molecular cavities *etc.*, the aggregation behavior is significantly disturbed. Consequently, the switching of excimeric to monomeric emission is a very natural and common strategy to monitor any analyte *in vitro* or *in vivo*. This makes pyrene derivatives highly desirable for bioimaging application which is one of the principal attractions of pyrene-based fluorophores. Additionally, pyrene is generally photostable under standard conditions, making it a reliable fluorescent marker in long-term experiments and applications. Since the fluorescence properties of pyrenes are susceptible to the surrounding solvent environment, they can also be employed to probe the polarity and microenvironment of the solvent or host matrix. These unique and versatile photophysical features of pyrene-based fluorophores attracted us to write a review article on their application in the fluorescence detection of heavy metal ions.[19]

In addition, pyrene is well known for its aggregation properties at the solution phase or solid state. Naturally, it is quite easy to expect that pyrene might cause either aggregation-induced emission (AIE) or aggregation-induced enhanced emission (AIEE) or aggregation-caused quenching (ACQ) upon preferential binding with an analyte. Also, polycyclic aromatic hydrocarbons like pyrene are highly electron deficient and pyrene derivatives containing an electron donor centre either conjugated or non-conjugated to the core might be involved in intramolecular charge transfer (ICT) or photoinduced electron transfer (PET) and even the

Nilanjan Dey

Dr. Nilanjan Dey obtained his Ph.D. degree in Supramolecular Chemistry from the IISC, Bangalore, India in 2017. Thereafter he joined as a JSPS postdoctoral fellow at Kyoto University, Japan. Then, he joined as an Assistant Professor at the Department of Chemistry of BITS-Pilani, Hyderabad, India. The current research interests of Dr. Dey are developing optical probes for biomolecules (proteins, carbohydrates, disease biomarkers, food toxins, and VOCs), investigating photochemical properties in confined media, designing vehicles for drug and gene delivery and developing responsive soft materials for biomedical applications. Dr. Dey has received several awards over the years, such as the Thieme Chemistry Journals Award in 2022, the NASI-Young Scientist Platinum Jubilee Award in 2022, and the MSCA-Seal of Excellence Award in 2021.

Michael Watkinson

Mike Watkinson studied undergraduate chemistry at the University of St. Andrews before relocating to UMIST to complete his Ph.D. in manganese Schiff base chemistry under the late Professor Noel McAuliffe for which the Royal Society of Chemistry presented him with the inaugural Laurie Vergnano Prize. In 1995, he was awarded a Royal Society Post-doctoral Fellowship, at the University of Santiago de Compostela in Spain. After completing his post-doctoral studies with Professor Andy Whiting at UMIST, he was appointed in 1998 to a lectureship at Queen Mary University of London. In 2018 he joined Keele University as the Head of the School of Chemical and Physical Sciences before joining Manchester Metropolitan University in 2024 as Deputy Pro-Vice Chancellor for the Faculty of Science and Engineering. The development of small molecule fluorescent probes for various sensing applications is the main focus of his present research.

Forster resonance energy transfer (FRET) process. Now, if any foreign analyte could selectively induce or tune either of these photophysical events, that particular foreign analyte could be recognized spectroscopically. This is one of the extensively utilized strategies of pyrene-based fluorophores. Besides, attachment of any hydrogen bond or proton acceptor centre or hydrogen bond or proton donor centre that might be involved in hydrogen bonding or proton transfer with a foreign analyte selectively might alter the photophysical properties of the pyrene derivative. In addition, the presence of multiple electron donor centres within a pyrene derivative might cause chelation enhanced quenching (CHEQ) or ligand to metal change transfer (LMCT) or metal to ligand charge transfer (MLCT) upon preferential binding with a particular metal ion. Naturally, there is a huge scope for pyrene derivatives to involve diverse photoprocesses in the fluorescence detection of diverse analytes of importance. During the discussion, we will find that different pyrene derivatives involve diverse photoprocesses in the detection of toxic cations like Ag^{+} and Pb^{2+}.[19]

Herein, our concern is the detection of two heavy metal ions, Ag^{+} and Pb^{2+}, from metals that have been used since Roman times and are closely associated as they were both mined from the same lead minerals galena (PbS) and lead carbonate. Heavy metals are mostly toxic even when present at very low concentrations. Despite this, heavy metals have a few positive effects like key roles in metabolism, catalysis and biomineralization, and some negative effects as a result of their high toxicity, causing serious health and environmental hazards.[20,21] Interestingly, various salts of Ag^{+} (silver nitrate, silver acetate, silver proteinate and silver sulphadiazine) can play a role in glycolysis, particularly in the production of lactate and pyruvate. Also, Ag^{+} has an important role in copper metabolism.[22,23] On the other hand, lead is widely used in the dye industry, gasoline and batteries and readily contaminates the environment, particularly soil and groundwater. Subsequently, it enters into the food chain and accumulates in biological cells and tissues.[24,25]

In spite of being used as a component of jewellery, ornaments and currency coins for millennia, silver has also been widely used in making utensils due to its bactericidal and disinfectant activities, in photography and in the electrical industry due to its high conductivity.[26–29] In addition, the minerals of silver (as Ag^{+} salts) exist in the Earth's crust and contaminate the environment due to mining activities and natural weathering. Contamination of Ag^{+} salts in the environment also occurs due to the extensive use of Ag^{+} salts in catalysts, electroplating, photography and medical devices (Fig. 1).[30] Despite such widespread applications, it is noted that the use of Ag^{+} ions has become more restricted in recent years due to environmental and health concerns associated with bioaccumulation and their toxicity.[31,32]

On the other hand, lead is one of the most toxic heavy metal elements and has contaminated food and drinking water due to its widespread historic use in batteries, plumbing, and paints, as an anti-knocking agent in gasoline,

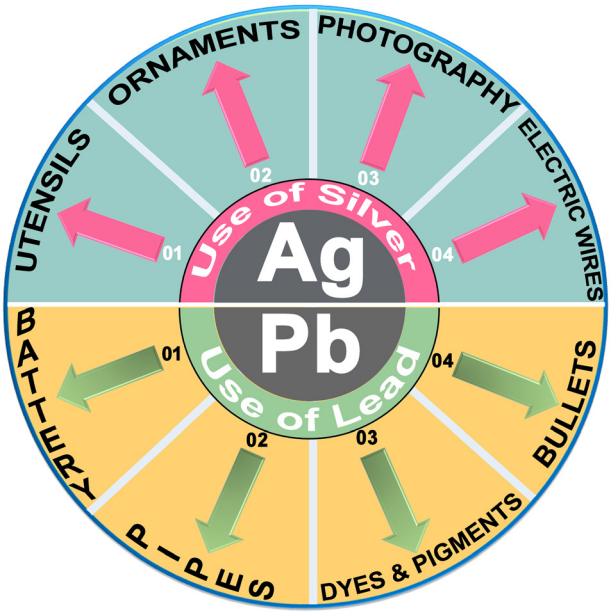

Fig. 1 Pictorial representation of the historical major uses of the metals silver and lead.

and in the dye industry to name but a few.[32,33] Considering its hazardous effects, the World Health Organization (WHO) has set a maximum permissible concentration of lead in drinking water (10 μg per litre).[34] Lead is extremely toxic and it causes long-lasting health issues even with minimal contamination and it can affect reproduction, slow down development, lead to cardiovascular disorders and can result in severe health issues in children, including poor IQ, slow motor response and hypertension.[35,36] It is therefore essential to take appropriate safety measures when working with silver or lead ions and their compounds, particularly in industrial settings or activities involving potential exposure. These measures include using personal protective equipment, ensuring proper ventilation, and following occupational health and safety guidelines. Additionally, it is crucial to ensure safe handling, storage, and disposal of silver and lead-containing materials to prevent environmental contamination and potential health risks to both humans and ecosystems.

The detection and quantification of silver and lead ions are essential in various fields, including environmental monitoring, industrial processes, and public health.[37,38] Traditional methods, such as atomic absorption spectroscopy (AAS),[39] inductively coupled plasma mass spectrometry (ICP-MS),[40] ion-selective electrodes (ISE),[41] X-ray fluorescence (XRF),[42] and electrochemical methods,[43,44] have been widely used to detect and measure the concentration of these ions in commercial setups. Most of these methods have fixed concentration ranges and sample matrices, which limit their applications in real-life sample analysis. Though it is very difficult to compare the cost-effectiveness, versatility, real-life applicability and analytical performance like selectivity, sensitivity, limit of detection, *etc.* of these methods for two particular heavy metal ions, a well-supported information table

was presented and discussed mentioning all these specifications of some of the above-mentioned techniques somewhere else.[45] Some methods are more suitable for high sensitivity and trace analysis but also need sophisticated high-end (and expensive) instrumental facilities, which can be very limiting for small and medium-sized companies. In contrast, optical sensors (either chromogenic or fluorometric) have many advantages over these conventional analytical techniques as they are mostly non-intrusive and non-destructive and exhibit high sensitivity and selectivity, which are especially beneficial for real-time monitoring, dynamic analysis, and detection of rapid changes in analyte concentrations in a complex matrix.[20,46] Optical sensing techniques can be easily adapted for multiplexing, allowing the simultaneous detection of multiple analytes in a single measurement, and are therefore suitable for high-throughput analysis. Not only that, recently, optical probes have been integrated with other technologies, such as microfluidics,[47,48] nanomaterials,[49,50] and smart devices,[51] to create advanced sensing platforms with improved performance and functionality.[52]

Given our ongoing interest in the development of pyrene-based fluorophores for the detection of an array of analytes of interest,[53–59] we focus this review article on the use of pyrene-based fluorophores in the optical detection of the heavy metals Ag^+ and Pb^{2+} ions. We focus on the recent developments of pyrene-based colorimetric and fluorescent sensors that have been successfully utilized in the highly selective and sensitive detection of Ag^+ and Pb^{2+} ions independently in non-aqueous, semi-aqueous and pure aqueous media. Moreover, the crucial application of these chemosensors for *in vivo* detection and imaging of the respective cations is also discussed.

Results and discussion

Colorimetric and fluorescence detection of Ag^+ ions by pyrene-based fluorophores

The design and development of heavy metal optical probes with high selectivity and sensitivity is challenging due to several essential salient structural and photophysical features. A model chemosensor must contain at least a metal binding or chelating unit and a signalling moiety, which may be connected directly or through a spacer. Herein, the signalling unit will be exclusively pyrene-based, but a variety of binding or chelating units are considered (Fig. 2).[21] If the chemosensor is a bright fluorophore and selective metal binding either decreases or increases the quantum yield, it might be beneficial for fluorescence imaging.[21] During the last two decades, there have been relatively few reports on the exploration of pyrene-based fluorophores as silver ion chemosensors and we discuss these as well as lead ion sensing and imaging events using various ligand architectures.

In 2002, to the best of our knowledge, for the first time, a pyrene-based chemosensor for the detection of Ag^+ ions was reported.[60] Kim and co-workers developed a series of calixarene-based fluoroionophores (**1–3**, Scheme 1) with crown and aza-crown ethers as distinct binding pockets so that the metal ions could coordinate to their preferred binding sites. It was interesting to note that a "molecular taekwondo" process was reported between the Ag^+ ions, followed by either K^+ or Cs^+ ions *via* distinct fluorescence responses, which could easily be implemented in selective recognition of the metal ions. Compound **2** displayed poor emission intensity. In contrast, upon binding with the Ag^+ ions, **2** displayed a sharp enhancement of emission intensity due to the inhibition of PET. Subsequently, the introduction of the K^+ ions displaced the Ag^+ ions just like the "coming in kicking out" fashion in a taekwondo fight and consequently the emission intensity was significantly diminished. Similar taekwondo-like behaviour was also observed with **1** *vs.* Cu^{2+}–K^+ ions and **3** *vs.* Ag^+–Cs^+ ions. From Job's plot measurements, it was observed that the probes only formed complexes of 1 : 1 stoichiometry with Ag^+ when bound to the aza-crown sites (Fig. 3). Such consecutive fluorometric responses were rare at that time and a significant development.

Ratiometric recognition of any analyte is always anticipated due to the additional advantage of internal referencing with minimum relative spectroscopic error.[61,62] In the ongoing progress towards the optical detection of Ag^+ ions, Yang *et al.* developed a pair of analogous pyrene-functionalized heterocyclic derivatives of which one (**4**, Scheme 1) could recognize Ag^+ selectively and efficiently *via*

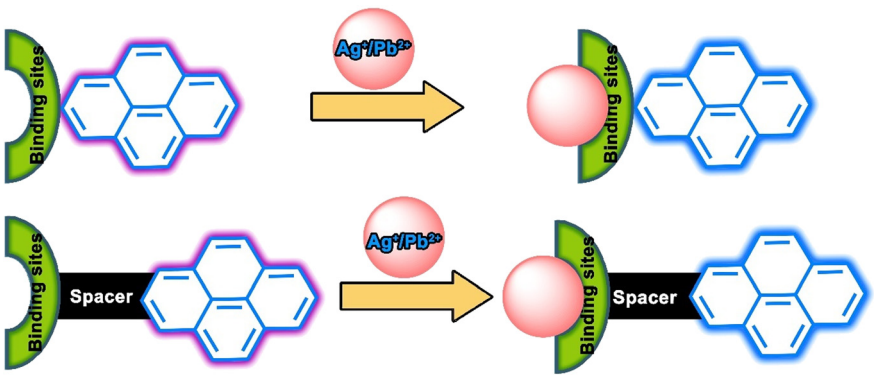

Fig. 2 Model structure of pyrene-based chemosensors for Ag^+ and Pb^{2+} ions and possible binding-driven signalling modes.

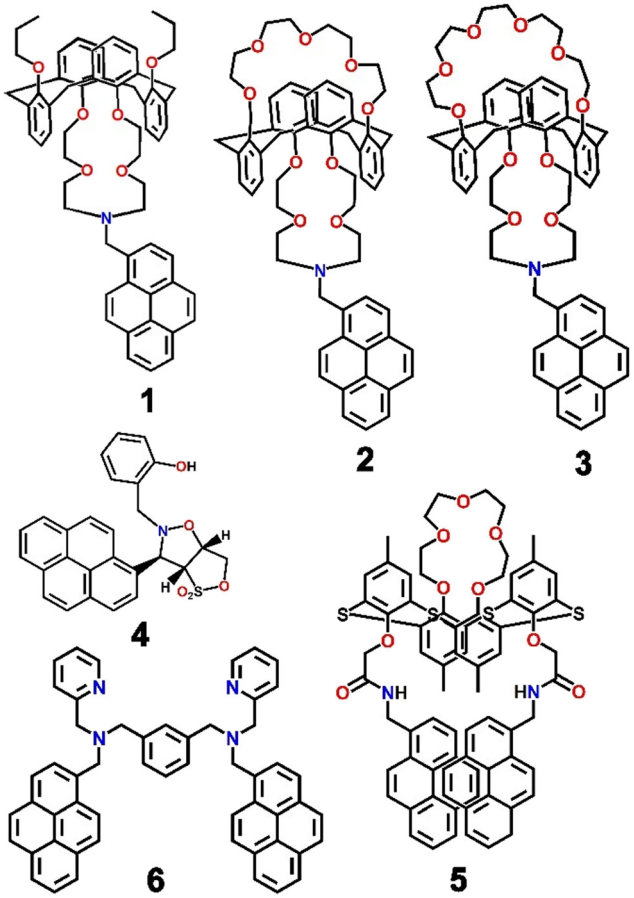

Scheme 1 Molecular structures of Ag^+ chemosensors **1**–**6**.

monitoring the ratiometric fluorescence changes in a highly polar protic medium (EtOH–H_2O; 1 : 1; v/v).[63] Heterocycle **4** was involved in the formation of a sandwich-type complex with Ag^+, thereby leading to ion-induced self-assembly of the fluorophore and a consequent significant increase in the fluorescence intensity of the excimer. Two emission bands were observed at 378 nm and 397 nm, upon excitation at 344 nm, due to typical pyrene monomeric emission behaviour. Upon binding with Ag^+, a red-shifted emission band at 462 nm was observed, probably due to typical pyrene excimer emission behaviour accompanied by a sharp isoemissive point at 412 nm, facilitating ratiometric detection. Such ratiometric and dual mode detection of Ag^+ ions was rare and a significant development in the field.

Shortly after Kim's report,[60] a similar type of chemosensor (**5**, Scheme 1) was designed by Kumar *et al.* by assembling two pyrene moieties with a thiacalix[4]arene moiety.[64] The chemosensor fluorometrically recognized both Ag^+ and Fe^{3+} ions *via* two different types of fluorescence responses. Ag^+ ions were detected by ratiometric fluorescence change whereas Fe^{3+} ions were detected by fluorescence quenching. Upon excitation at 344 nm, **5** displayed weak monomeric and strong excimer emission signals of the pyrene moiety at 377 nm and 470 nm, respectively; however, upon gradual addition of Ag^+, the band at 470 nm was quenched and fluorescence enhancement at 377 nm was simultaneously observed. In contrast, the quenched emission of **5** in the presence of Fe^{3+} was only recovered by the addition of cysteine. Most interestingly, the reversible and reproducible fluorescence responses of **5** in the presence and/or absence of Ag^+, Fe^{3+} and cysteine were implemented in the configuration of the Set/Reset opto-chemical logic designed feedback loop with a very useful "Write–Read–Erase–Read" feature (Fig. 4).

In the same calendar year, another fluorescent probe was synthesized by anchoring two pyrene and pyridine units (**6**, Scheme 1) that recognized Ag^+ ions ratiometrically by monitoring the monomer and excimer emission of the pyrene units.[65] In HEPES buffered DMSO medium (1 : 1; v/v; pH = 7.2), the probe displayed a monomeric emission band at 399 nm along with an excimer band at 463 nm (λ_{ex} = 344 nm). This event clearly revealed the presence of π–π interactions. Unlike the behaviour observed with other cations tested, upon the gradual addition of Ag^+, the monomeric emission band of the probe was concomitantly promoted with a simultaneous decrease of the excimer emission. Extensive DFT calculations and ^1H NMR

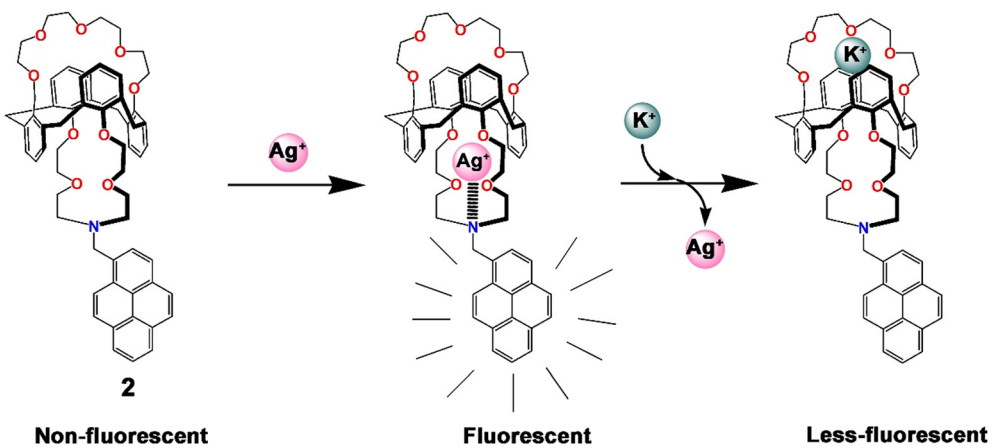

Fig. 3 Pictorial representation of the probable mode of sequential binding of **2** with Ag^+ and K^+ ions.[60]

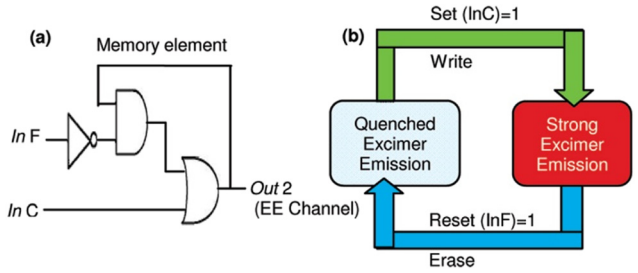

Fig. 4 Graphical depiction of a sequential logic circuit (a) and memory element with a useful "Write–Read–Erase–Read" feature (b) (reprinted with permission from ref. 64. Copyright 2011, American Chemical Society).

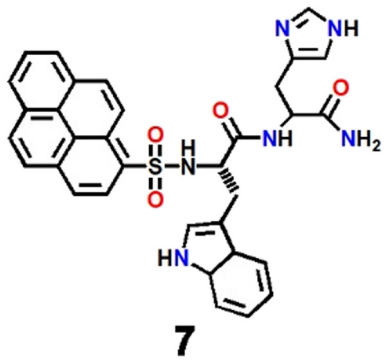

Scheme 2 Molecular structure of probe 7.

spectroscopic titration clearly revealed the involvement of the nitrogen atoms in the coordination of the Ag^+ ions in the 1:1 complex formation.

Thereafter, a pyrene-dipeptide-based fluorescent probe (7, Scheme 2) was developed by Jang *et al.* and established its role as a selective and ratiometric sensor for Ag^+ as well as silver nanoparticles in water at physiological pH.[66] The probe displayed emission bands at 378 nm and 395 nm due to the typical monomeric form of pyrene. The peaks concomitantly diminished with the development of a new signature emission band at 480 nm in the presence of Ag^+. The probe formed an excimer in the presence of Ag^+ that could easily be recognized *via* a typical excimer band at 480 nm with high fluorescence emission. Chemosensor 7 was shown to be capable of detecting intracellular Ag^+ in live cells through strong ratiometric signals (Fig. 5). Such ratiometric detection of silver ions as well as nanoparticles *in vivo* and *in vitro* was a major advance in the field of Ag^+ ion sensing.

Wang *et al.* synthesized a series of calix[4]arene-based chemosensors, two of which contained pyrene and non-conjugated triazole moieties on the lower-rim of the calix[4] arene (**8** and **9**, Fig. 6) and showed excellent ratiometric fluorescence responses towards Ag^+ with excellent sensitivity even in MeOH–$CHCl_3$ (98:2; v/v) mixed solvent.[67] When excited at 342 nm, the probe exhibited strong emission peaks at 379 nm and 398 nm for monomer emission and at 476 nm for excimer emission. In the presence of Ag^+, the monomeric emission bands of **8** at 379 and 398 nm were gradually enhanced with a simultaneous decrease of the excimer emission band. In contrast, **9** displayed an enhancement of emission intensity of both the monomer and excimer emission bands in the presence of silver ions. In addition, both the probes formed a 1:1 complex with Ag^+ and the binding mechanism was well justified with ^1H NMR

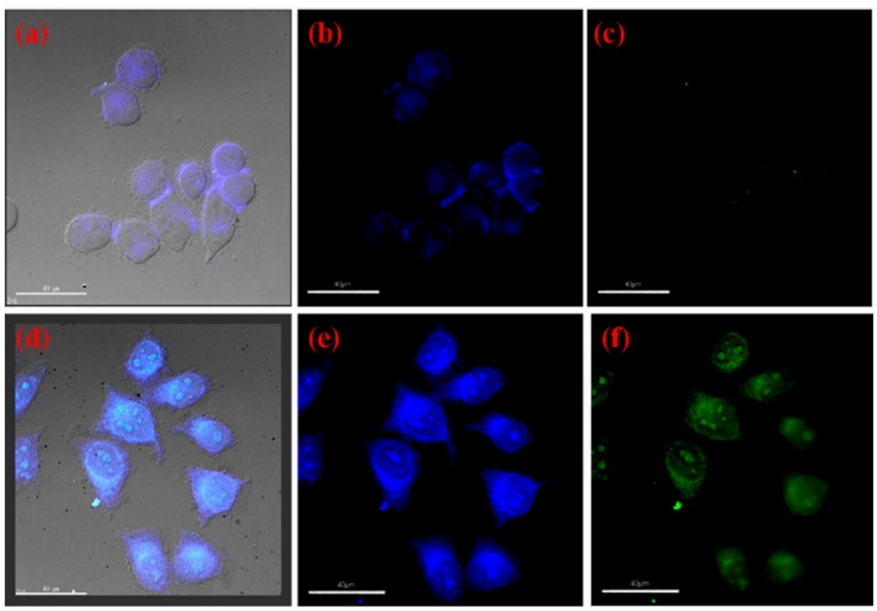

Fig. 5 The fluorescence images of living cells (HeLa) incubated with 7 in the absence (a–c) and presence of Ag^+ (d–f) under a wide range of different experimental conditions; bright field fluorescence images (a and d), λ_{em} = 435 ± 48 nm (b and e), and λ_{em} = 523 ± 35 nm (c and f); (reprinted with permission from ref. 66. Copyright 2012, American Chemical Society).

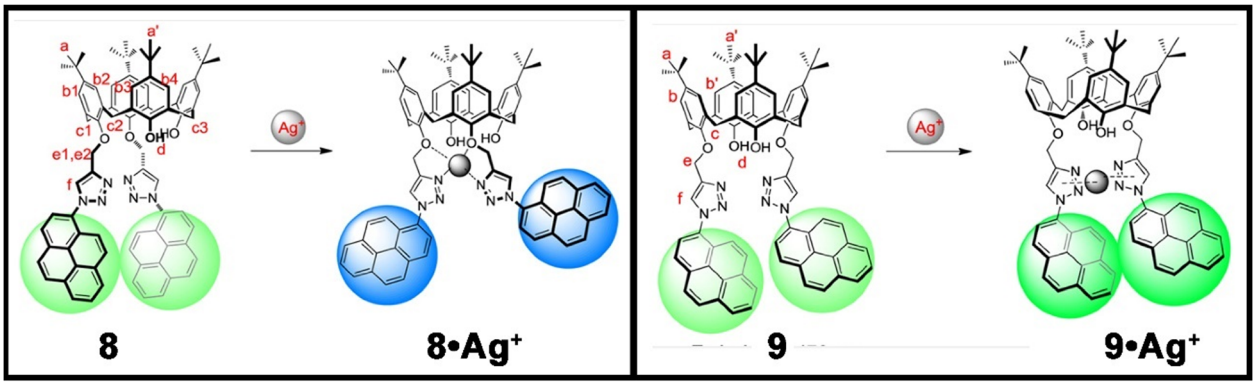

Fig. 6 The binding mechanism and 1 : 1 complex formation of probes **8** and **9** with Ag^+ ions (reprinted with permission from ref. 67. Copyright 2012, Elsevier).

spectroscopic titration. Interestingly, the probe was operative even in the presence of an aqueous methanol medium. Unfortunately, both probes also responded to Cu^{2+} and Hg^{2+} ions resulting in poorer selectivity.

Later, Lodeiro *et al.* extended the synthesis protocol with a pyrene-based ligand system. The group synthesized two novel fluorescent probes bearing one and two pyrene unit-containing derivatives (**10** and **11**, Fig. 7) which efficiently recognized water and Ag^+, as well as Cu^{2+} and Zn^{2+} ions, in dioxane medium.[68] In addition to distinct spectroscopic changes, all three metal ions were distinguished with remarkable naked-eye colour changes. Interestingly, **10** displayed a higher affinity for Cu^{2+} whereas **11** was more responsive to Ag^+. The development of such pyrene-based fluorophores with the capability to recognize and discriminate Ag^+ was a significant development for real-life applications.

In continuation of their previous study,[65] a new pyrene–pyridine anchored gibbet-based fluorescent chemosensor (**12**, Fig. 8) was demonstrated to be selective and sensitive (LOD = 2.9 nM) for the detection of Ag^+ in HEPES buffered DMSO–H_2O (1 : 1, v/v; pH = 7.4) mixed solvent by monitoring the fluorescence "on–off" of the probe.[69] In its free state, the probe displayed both monomeric and excimeric emissions. But when bound to Ag^+, the formation of the excimer of the probe was restricted and PET from the metal-bound pyridine to the pyrene moiety was enhanced by the rigidity of the probe turning it into a butterfly-like skeleton, which in turn quenched the monomeric emission (Fig. 8). The probe was shown to be able to estimate the metal ion concentration in Ag^+ spiked local water samples with excellent accuracy.

Chang *et al.* synthesized a probe (**13**, Fig. 9) having several binding possibilities with different analytes and used it to detect silver ions, formaldehyde and fructose.[70] The probe utilised a number of binding interactions such as a dynamic covalent interaction between a diol and boronic acid, silver ion and pyridyl ligand, through a coordination interaction and an easily accessible reaction possibility between the secondary amine and formaldehyde with pyrene as the fluorophore. Compound **13** reacted with fructose and formed a blue coloured fluorescent adduct that further reacted with Ag^+ to form a 2 : 1 complex with the pyridyl residues with a change in solution colour from blue to green. The complete and multiple binding motifs of the probe in different dynamic states with different analytes along with the fluorescent colour changes are presented in Fig. 9.

A new technique has been developed by Zhang *et al.* to selectively detect silver ions using supramolecular assembly of a water-soluble pyrene derivative (**14**, Scheme 3) and cucurbit[10]uril.[71] The 1 : 1 host–guest type inclusion complex recognized Fe^{3+} and Ag^+ ions independently. In the presence of Ag^+, the composite displayed an enhancement of emission intensity at 332 nm due to an alteration of the ICT character and the fluorescence change was observed in confocal

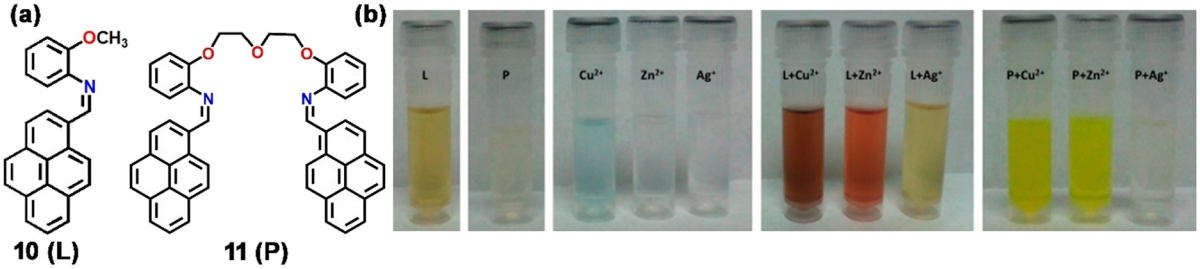

Fig. 7 (a) Molecular structure of the probes **10** (designated as **L** in the original article) and **11** (designated as **P** in the original article); (b) the naked-eye colour of the probes, metal ions and probe–metal ion complexes in the solution phase (reprinted with permission from ref. 68. Copyright 2013, American Chemical Society).

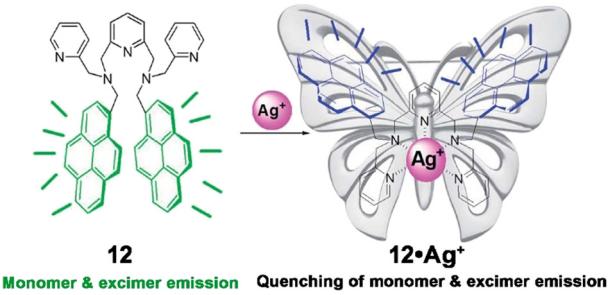

Fig. 8 Binding motif of **12** and the development of a rigidity enhanced butterfly-like skeleton with Ag^+ (reprinted with permission from ref. 69. Copyright 2014, The Royal Society of Chemistry).

microscopy images (Fig. 10). Remarkably, the sensor system was extremely selective towards these metal ions over 37 other metal ions. Application of such a host–guest type inclusion complex as an Ag^+ ion sensor was new, rare and innovative.

In 2020, Lavado *et al.* synthesized and characterized a pair of calix[4]arene based sensors (**15** and **16**, Scheme 4) with thiourea as a spacer and pyrene or methylene–pyrene as the fluorophore, which selectively recognized silver ions with nanomolar scale sensitivity.[72] In a UV-vis spectroscopic study, **15** showed a defined band at 280 nm and two other overlapping bands at 332 and 347 nm in an acetonitrile–DMSO (99 : 1) solvent mixture. In the emission spectra, **15** displayed a band at 406 nm whilst **16** showed three bands at 377, 395, and 472 nm. Upon inclusion of Ag^+, **15** showed a sharp quenching of fluorescence intensity at 406 nm, whereas **16** exhibited a totally different decrease of the pyrene excimer band at 472 nm. The sensitivity was remarkable, but both the probes suffered from selectivity issues with Hg^{2+}

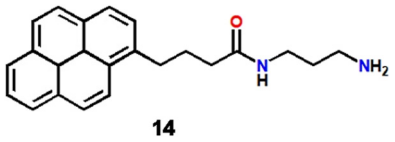

Scheme 3 Molecular structure of **14**.

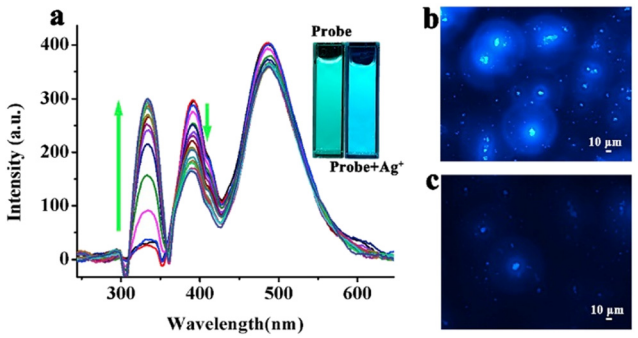

Fig. 10 (a) Fluorescence spectral changes of **14** with gradual addition of Ag^+; confocal images of **14** in the absence (b) and presence of Ag^+ (c) (reprinted with permission from ref. 71. Copyright 2020, Elsevier).

ions, which also quenched fluorescence. Interestingly, using chemical inputs and respective emission spectral results, several useful opto-chemical logic gates like INHIBITION and IMPLICATION were designed.

Very recently, Ju *et al.* synthesized a pair of argentivorous fluorophores (**17** and **18**, Scheme 4) containing anthracenyl– or pyrenyl–benzyl moieties.[73] Probe **17** showed a bright emission at 506 nm (ϕ = 0.46) but its emission was significantly reduced (ϕ = 0.16) in the presence of silver ions (Fig. 11). This quenching event was initiated due to the PET from the amine to the nearby anthracene moiety. On the

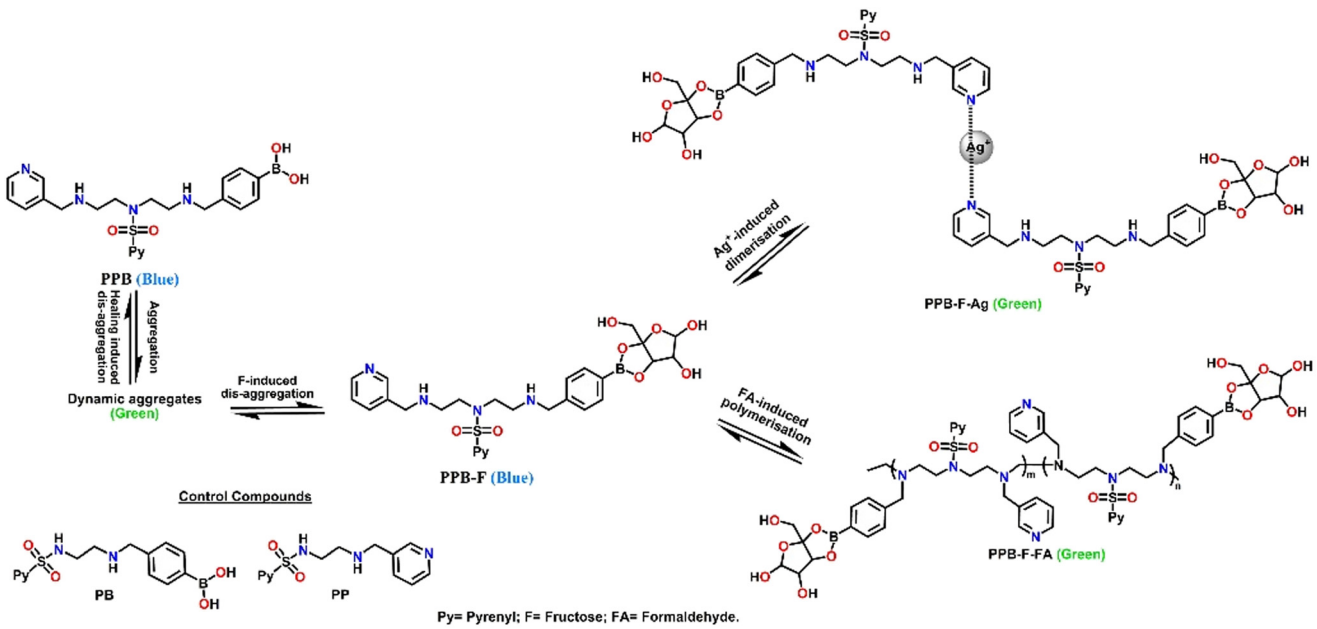

Fig. 9 Pictorial representation of the relevant states of the dynamic molecular system **13** in the presence of different analytes.[70]

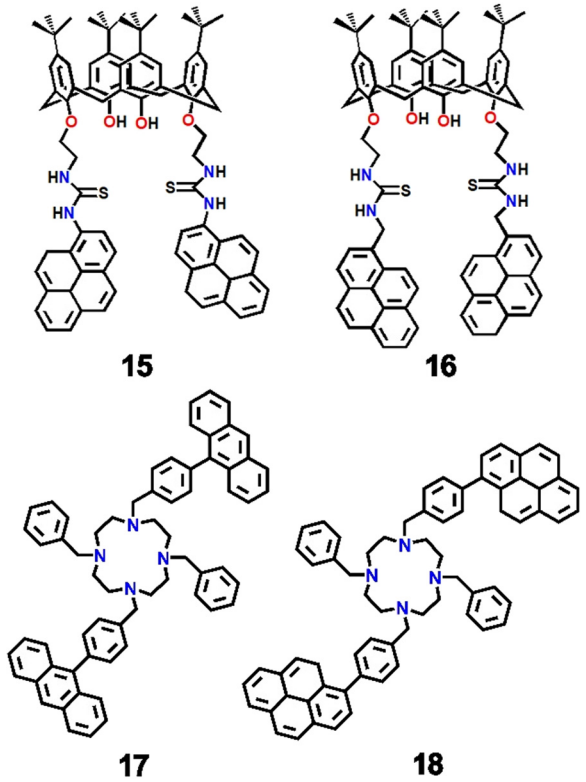

Scheme 4 Molecular structures of Ag^+ chemosensors **15**–**18**.

other hand, probe **18** displayed a weak blue emission at 409 nm (ϕ = 0.14) but that was changed suddenly in the presence of Ag^+ with bright blue luminescence at 462 nm (ϕ = 0.40) being observed. The poor fluorescence emission of **18** was attributed to PET from the nitrogen atom of the cyclen moiety to the excited pyrene moiety. The inclusion of the Ag^+ ion was proposed to inhibit the PET and enhanced rigidity due to the CHEF effect also boosted the fluorescence intensity sharply. Interestingly, the report established the structure–fluorescence change relationship for the cyclen-based receptor.

The above examples demonstrate the colorimetric and fluorescence detection of Ag^+ ions by pyrene-based fluorophores, which in most cases utilise architectures in which the pyrene was tethered with either pyridine or calix[4]arene moieties. In a few cases, amines or substituted amines were integrated with pyrene moieties. The nitrogen centres of all these pyrene-based fluorophores were involved in selective coordination with Ag^+ and altered either the monomer–excimer emission behaviour, PET phenomenon or chelation-enhanced fluorescence behaviour. Fluorophore–cucurbit[10]uril host–guest inclusive complexation was also employed as a chemosensing mechanism. Few of the chemosensors, however, were able to recognize Ag^+ by naked-eye colour change. Nonetheless, the ion-induced spectroscopic responses observed were utilized in the development of opto-chemical logic gates and memory devices in several cases. Unfortunately, it was observed that most of the Ag^+ ion chemosensors failed to distinguish the Hg^{2+} ion.

Finally, a sensor information table for the Ag^+ sensors discussed above containing basic information like the binding unit, medium, nature of fluorescence response, photo-process involved, LOD, and any special features is presented, Table 1.

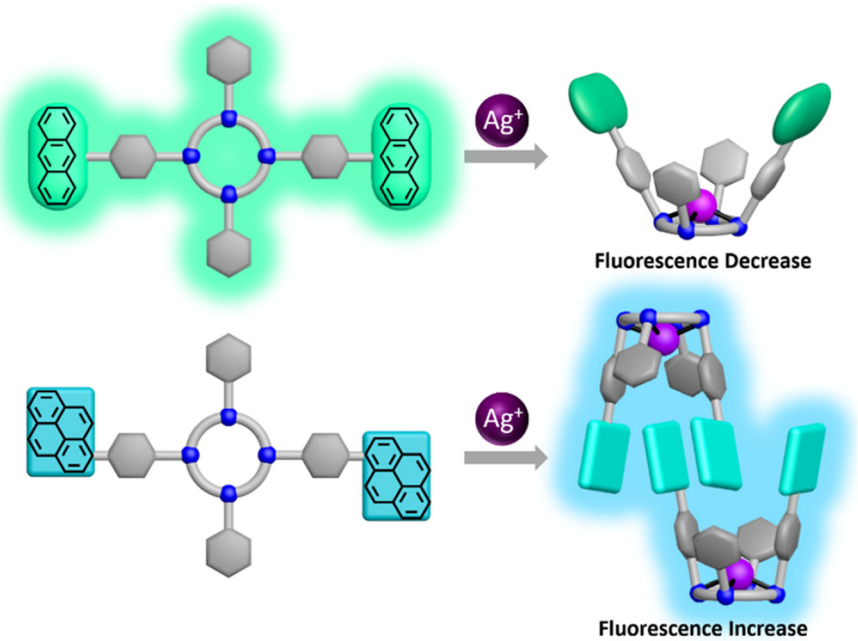

Fig. 11 Pictorial representation of the binding motifs of the probes **17** and **18** with the Ag^+ ion (reprinted with permission from ref. 73. Copyright 2021, American Chemical Society).

Table 1 Sensor information table for Ag^+ ion sensors containing the binding unit, medium, nature of fluorescence response, photo-process, LOD and any special features

Binding unit	Medium	Fluorescence response	Photoprocess	LOD	Special feature	Ref.
Calixarene-based crown ether & aza-crown ether (**1–3**)	EtOH	Turn on	Inhibition of PET and CHEF	—	"Molecular taekwondo" between metal ions	60
Heterocyclic macrocycle (**4**)	EtOH–H_2O; 1 : 1; v/v	Ratiometric	Formation of an excimer	—	Ion-induced self-assembly driven formation of an intramolecular sandwich complex	63
Thiacalix[4]arene (**5**)	10% aqueous ethanol	Ratiometric	Conformational change	—	Configuration of Set/Reset opto-chemical logic designing in a feedback loop with a very useful "Write–Read–Erase–Read" feature	64
Bispyrene–pyridine derivative (**6**)	HEPES buffered DMSO	Ratiometric	Inhibition of ICT	—	Monomer–excimer switching	65
Histidine-tryptophan dipeptide (**7**)	Aqueous solution containing 1% DMF	Ratiometric	Formation of an excimer	—	*In vivo* detection of Ag^+ within HeLa cells	66
Calix[4]arene-triazole derivative (**8** and **9**)	MeOH–$CHCl_3$ (98 : 2; v/v)	Ratiometric	CHEF	—	Interconversion between dynamic and static excimers	67
Aminophenoxy-oxopentane (**10** and **11**)	Dioxane	Quenching	Monomer to dimer conversion	—	Prominent naked-eye color change	68
Pyridine derivative (**12**)	HEPES-buffered DMSO–H_2O	"Turn off"	PET	2.9 nM	Butterfly like architecture	69
Pyridine-boronic acid-fructose adduct (**13**)	Carbonate buffered DMSO	Ratiometric	Formation of an excimer	2.5 μM	Aggregation–disaggregation	70
Aminopropyl-pyrene derivative-cucurbit[10]uril inclusion complex (**14**)	H_2O	Enhancement of fluorescence intensity	ICT	—	Inclusion complex as a chemosensor	71
Calix[4]arene-thiourea derivative (**15** and **16**)	MeCN–DMSO (99 : 1; v/v)	Quenching of excimer emission	Through bond and cation–π interaction	2.09 nM	Decoration of INHIBITION and IMPLICATION opto-chemical logic gates	72
Tetra-armed cyclens (**17** and **18**)	—	"Turn on"	PET & CHEF	—	Detection of ions in the solid state	73

Colorimetric and fluorescence detection of Pb^{2+} ions by pyrene-based fluorophores

During the previous two decades, concerns about lead as an environmental pollutant have been widespread. The development of fluorescent probes for this toxic heavy metal ion with sufficient selectivity and sensitivity has been an area of much attention and several scientific groups have contributed significant effort in the development of effective fluorescent sensors for this pernicious analyte. In this regard, pyrene moiety-based sensors have been major stakeholders with a range of different ligand topologies.

In 2004, Kim *et al.* developed a pair of new fluorescent sensors (**19** and **20**, Scheme 5) with two pyrene moieties linked to a cation recognition unit of a 1,3-alternate calix[4] arene framework that selectively recognized Pb^{2+} and K^+ ions. The probe formed an excimer in solution that displayed an emission band at 470 nm, which was quenched by Pb^{2+} but subsequently revived by the addition of K^+.[74] Two pyrene moieties with a cation recognition unit made of an amide linkage created a potent monomer and excimer in the free ligand. When metal ions were added, the emission spectral behaviour was entirely changed. Whilst **19** was highly selective towards both Pb^{2+} and K^+ individually and sequentially in a reversible manner, **20**, which had propyl groups in place of the crown-5 ring, had high selectivity only for Pb^{2+}. Both the monomer and the excimer bands were significantly quenched upon the addition of Pb^{2+} to a solution of **19** in MeCN solution because of reverse PET from the pyrene group to the amide group. It was important to note that when K^+ was introduced to a solution of **19**, the emission behaviour remained unaltered because K^+ was trapped by the crown-5 ring rather than the amide group.

The same group also developed another pair of new fluorogenic calix[4]arene-based chemosensors (**21** and **22**, Scheme 5) containing triazacrown-5 with two pyrenyl amide groups that can be used for both cation and anion-selective chemo-sensing purposes.[75] While compound **21** emitted at 448 nm, compound **22** emitted at 472 nm. The difference of 24 nm blue shifted emission between the two compounds was due to the triazacrown ring's steric hindrance across the two pyrene pendants. When Pb^{2+} or Co^{2+} was introduced to **22**, the fluorescence intensities were quenched due to the effects of the metals, reverse PET, and conformational changes. The two pyrenyl amide groups contributed significantly to the selective Pb^{2+} ion complexation by using an azacrown unit. Interestingly, the **21**–Pb^{2+} composite also

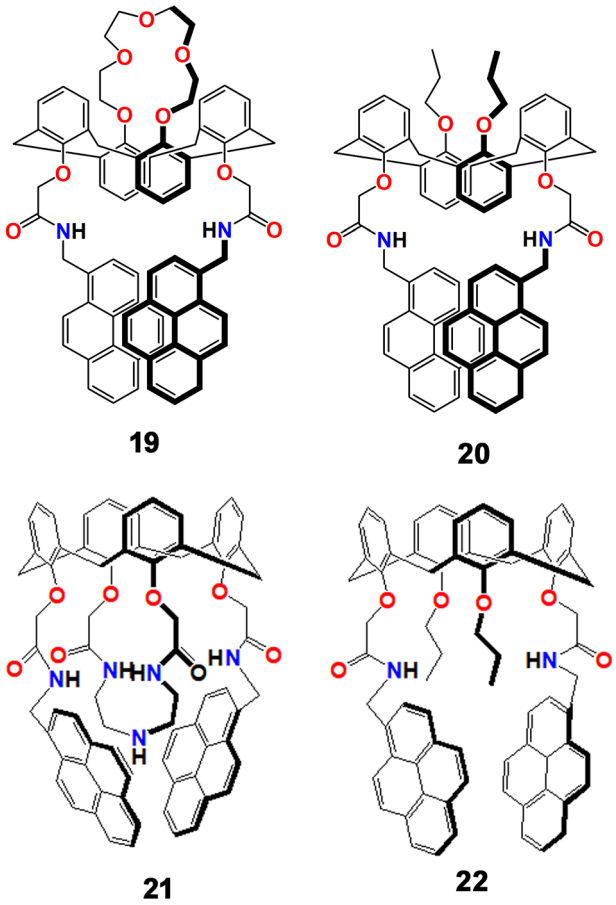

Scheme 5 Molecular structures of Pb^{2+} ion chemosensors **19**–**22**.

recognized fluoride ions driven by anion selective hydrogen bonding interactions.

In a different study by the same group, three pyrene derivatives were developed by assembling calix[4]arenes connected with a pendant like ethyleneamine on their triazacrown ring (**23**–**25**, Scheme 6).[76] Compounds **23** and **24** displayed weak monomer and excimer emission bands at 396 nm and 467 nm, respectively (λ_{ex} = 343 nm), due to PET from the hanging pendant-like $-CH_2CH_2NH_2$ moieties appended to the fluorogenic pyrenes. In contrast **25**, which did not contain these pendant-like moieties, displayed strong monomer and excimer emission. When Pb^{2+} was added to a MeCN solution of **23** and **24**, the monomer emission increased gradually, while the excimer emission was diminished simultaneously. However, for **25** both the monomer and excimer emissions were decreased significantly upon binding with Pb^{2+}. This was because of the carbonyl bond change in orientation and the primary amine being involved in the three-dimensional encapsulation. The quenching of excimer emission of **23** and **24** was attributed to inhibition of PET due to involvement of the $-CH_2CH_2NH_2$ moiety coordinating with Pb^{2+}, disfavouring excimer formation. But for **25**, the C═O···Pb^{2+} coordination and subsequent conformational changes initiated the quenching of excimer emission, whereas the heavy metal ion effect and reverse-PET collectively originated the monomer quenching. Moreover, **23** and **24** displayed high selectivity and sensitivity towards fluoride ions.

In 2006, Choi *et al.* devised a pair of pyrene-based fluoroionophores (**26** and **27**, Scheme 7), one of which contained two cation recognition sites (a crown ether ring and two facing pyreneamide groups) and displayed different chemosensory responses with two transition metal ions, Pb^{2+} and Cu^{2+}, and one alkali metal ion, K^+. In these multiple metal ion detection events, photoinduced charge transfer (PCT) was reported to take a crucial role in producing distinguishable spectroscopic patterns.[77] Both the compounds displayed monomer (λ_{em} = 384 nm) as well as excimer (λ_{em} = 484 nm) emissions upon illumination at 343 nm in acetonitrile solution. The monomer and excimer emissions of **26** were quenched in the presence of both Cu^{2+} and Pb^{2+} due to reverse PET and conformational changes. The Pb^{2+} ion was proposed to be bound to two adjacent amide oxygen atoms of **26** and not with the crown ether ring, as control compound **27**, which did not contain the crown ether ring, also displayed similar quenching of both monomer and excimer emission bands upon inclusion of Pb^{2+}. However, the observed spectral changes upon the addition of K^+ ions were different. Upon binding with K^+, **26** displayed enhancements of the excimer emission band, probably

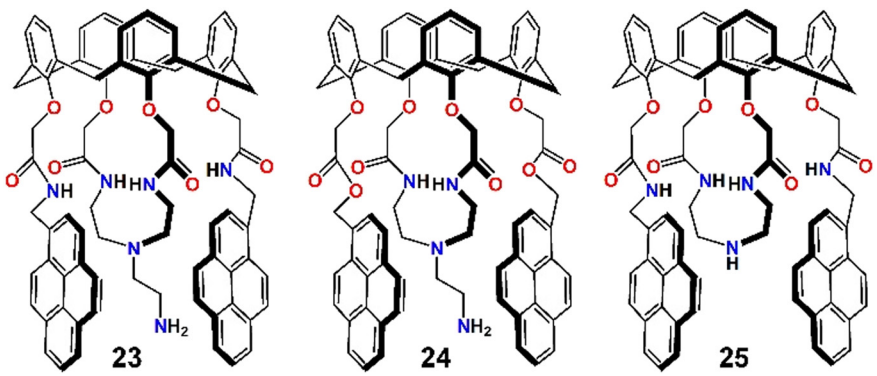

Scheme 6 Molecular structures of Pb^{2+} ion chemosensors **23**–**25**.

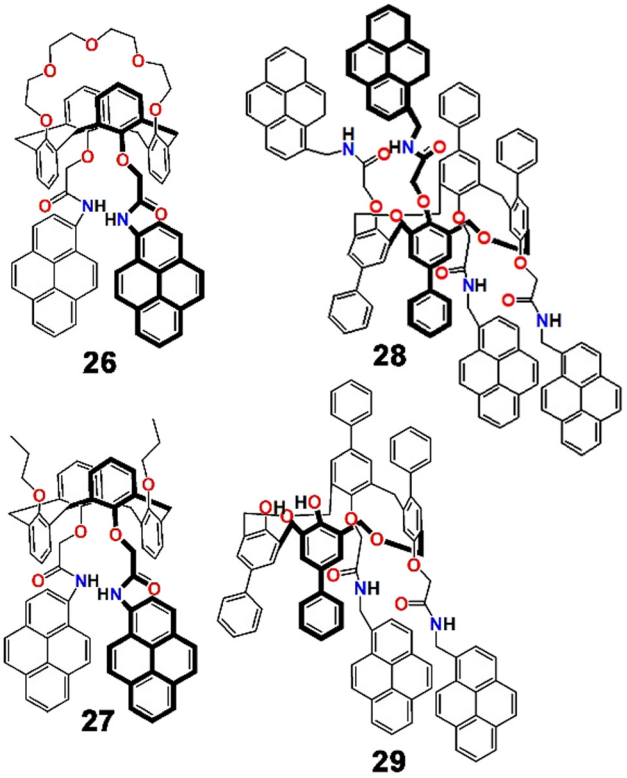

Scheme 7 Molecular structures of Pb^{2+} ion chemosensors **26**–**29**.

due to binding at the crown ether ring. Interestingly, **26** displayed exchanges of cations with consecutive addition of Pb^{2+} followed by K^{+} ions due to electrostatic repulsion between two metal ions. This work was not only important from a fluorescence detection point of view but also for the ion-exchange phenomenon (Fig. 12).

In the same year, the group also reported another pair of tetrahomodioxacalix[4]arene-pyreneamide tethered pyrene derivatives (**28** and **29**, Scheme 7), which selectively and efficiently recognized Pb^{2+} and Ca^{2+} ions in $CHCl_3$–MeCN (1 : 3; v/v) mixed solvent.[78] While Ca^{2+} ion binding caused the receptor to produce an elevated excimer and a decreased monomer emission with a ratiometric response, Pb^{2+} coordination resulted in quenched monomer and excimer fluorescence emission. Frontier molecular orbital analysis of **29** established the variations in excimer emission spectra by explaining why the effective π–π* interaction caused an increase in emission intensity upon Ca^{2+} ion complexation, but not upon Pb^{2+} binding. Coordination between **29** and Pb^{2+} disfavoured the formation of H-bonding in the pyrenyl amide moieties and consequently discarded the possibility of Py–Py* interactions and resulted in quenched excimer emissions.

Later, Kumar *et al.* synthesized a trio of analogous calix[4]arene-pyrene assembled fluorophores (**30**–**32**, Scheme 8) and

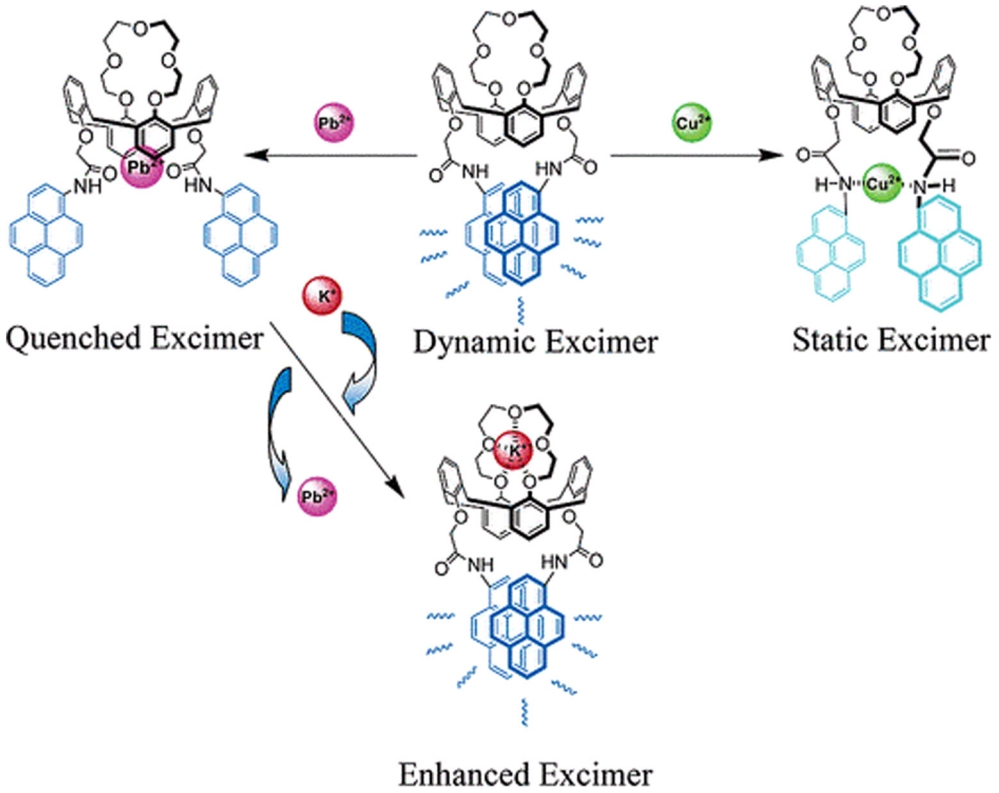

Fig. 12 Pictorial representation of the binding motifs of the probe **26** with Cu^{2+}, Pb^{2+} and K^{+} ions (reprinted with permission from ref. 77. Copyright 2006, American Chemical Society).

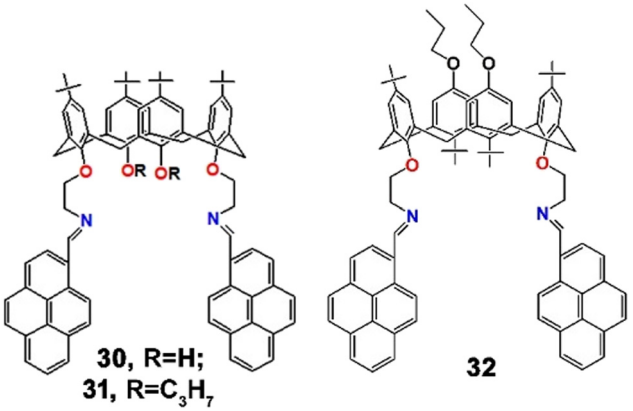

Scheme 8 Molecular structures of Pb^{2+} ion chemosensors **30**–**32**.

established their selective binding ability towards Pb^{2+} over other various metal ions in CH_2Cl_2 : MeCN (1 : 1; v/v) mixed solvent.[79] Interestingly, the probes **30** and **31** showed ratiometric spectroscopic changes but **32** only displayed "on–off" behaviour upon binding with Pb^{2+}. In an absorption study, **31** showed typical absorption bands at 363, 372, and 393 nm. Upon addition of Pb^{2+} to the solution of **31**, the absorption band due to the aza-bridge at 363 nm gradually decreased with simultaneous formation of a new red-shifted absorption band at 451 nm through the intermolecular charge transfer phenomenon (ICT). Also, with the incorporation of Pb^{2+}, **31** displayed a ratiometric shift of emission spectra, through an increase of the excimer band at 502 nm and a decrease of the monomer band at 407 nm. The reverse PET process to the imine nitrogen from the photoexcited pyrene was proposed to be responsible for the monomer quenching, and simultaneous conformational rigidity due to metal complexation resulted in the augmentation of the excimer band. On the other hand, **32** displayed strong quenching of its excimer band at 486 nm due to a reverse PET process. In addition, the 1 : 1 binding stoichiometry and sub-nanoscale detection limit (LOD = 490, 100 and 290 nM for **30**, **31** and **32**, respectively) were also determined. Such diverse behaviour of analogous fluorophores towards a particular metal ion was very interesting.

On the backbone of homooxacalix[3]arene, a pair of entirely novel types of fluorescent chemosensors (**33** and **34**, Scheme 9) that recognized Pb^{2+} ions in MeCN : H_2O : DMSO (1000 : 50 : 1; v/v/v) mixed solvent were reported by Ni *et al.* The group established far better chemosensory behaviour of **34** over **33** towards Pb^{2+}.[80] Gradual addition of Pb^{2+} resulted in a ratiometric shift of emission bands of **34**. When excited at 343 nm, the monomeric emission band of **34** at 396 nm was promoted with a simultaneous decrease of the excimer emission band upon complexation with Pb^{2+} ions. Such a ratiometric fluorescent chemosensor for the heavy metal ion with the homooxacalix[3]-arene C_3 symmetric structure displaying ratiometric enhancement of monomeric emission was very unusual at this time.

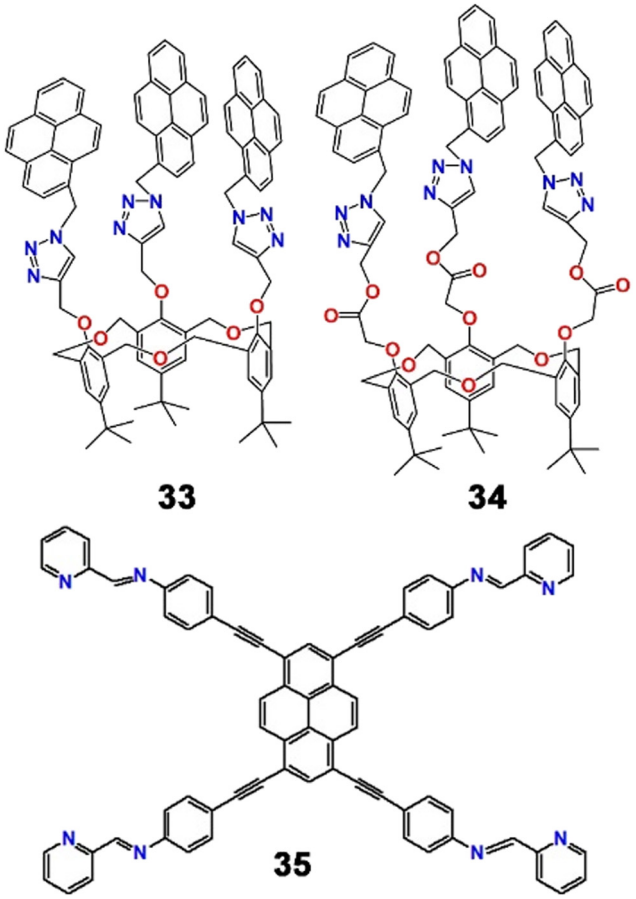

Scheme 9 Molecular structures of Pb^{2+} chemosensors **33**–**35**.

Later, Wang *et al.* developed a pyrene–pyridine-based fluorescent Schiff base connected by acetylenic linkers (**35**, Scheme 9) that selectively recognized Pb^{2+} and Ni^{2+} ions independently in DMF–H_2O mixed solvent.[81] Remarkably, the chemodosimeter was visible light excitable and exhibited fluorescence "on–off" responses in the presence of Ni^{2+} and "green–red" fluorescence switching upon binding with Pb^{2+} with different response times. Upon excitation at 460 nm, **35** displayed strong emission bands at 509 nm and 545 nm (φ = 0.438). The addition of Pb^{2+}

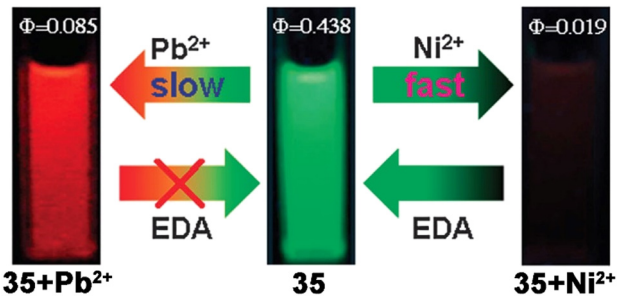

Fig. 13 Pictorial representation of different binding motifs of **35** with Ni^{2+} and Pb^{2+} ions with corresponding fluorescent colour changes and quantum yield values (reproduced with permission from ref. 81. Copyright 2012, The Royal Society of Chemistry).

to the solution of **35** not only reduced the emission intensity (φ = 0.085) but also increased the intensity ratio (I_{545}/I_{509}) from 0.334 to 1.114. Notably, the reaction time for Pb^{2+} was delayed in comparison with the Ni^{2+} ion, which might be a tool to distinguish the cations. Such a fluorescent probe could therefore demonstrate two new, highly effective ways for differentiating between Ni^{2+} and Pb^{2+} ions through different binding behaviours of the "*in situ*" produced Ni^{2+} and Pb^{2+} complexes with ethylene diamine (EDA) (Fig. 13).

Thereafter, Oton *et al.* developed three ferrocene-triazole tethered derivatives with a variable aromatic moiety by tandem click/Staudinger–aza Wittig reactions.[82] Among the three derivatives produced, the Pb^{2+} sensing properties of pyrene derivative **36** were explored by electrochemical and spectroscopic methods in $MeCN:CH_2Cl_2$ (4 : 1; v/v) mixed solvent. Upon interaction with Pb^{2+}, the absorption band of the probe displayed a ratiometric blue shift from 382 to 347 nm accompanied by a yellow to yellowish red colour and a sharp increase of emission intensity (φ = 0.027) from a very poor fluorescence emission ($\varphi < 0.001$). Such enhancement of emission intensity was attributed to a CHEF process (CHEF = 125). Hitherto, heavy metal ions like Pb^{2+} have mostly exhibited quenching of emission intensity as their detection method, and such "turn on" based detection was very rare.

In 2013, Neupane *et al.* synthesized a pyrene-tryptophan tethered fluorophore (**37**, Scheme 10) that fluorimetrically recognized Pb^{2+} *via* a "turn on" response of the monomeric band at 380 nm and Hg^{2+} *via* "turn on" responses of both the monomeric (380 nm) and excimeric bands (475 nm) in HEPES buffered aqueous solutions (pH = 7.4).[83] The probe **37** itself showed typical weak emission bands at 378 nm and 395 nm. The poor emission was due to PET from the tryptophan to the pyrene moiety. The binding of Pb^{2+} with the indole group impeded the PET process with the consequential enhancement of monomeric emission of the pyrene moiety. The exclusive role of the tryptophan moiety as a ligand and a quencher for recognition and fluorescence changes upon metal binding has not been explored previously.

Thereafter, Thakur *et al.* synthesized two pairs of electrochemical and optical sensors (**38–41**, Fig. 14) by assembling ferrocene–triazole–anthracene and ferrocene–triazole–pyrene (one pair each) *via* click reactions.[84] In addition to electrochemical responses, the probes exhibited significant promotion of the characteristic emission band upon binding with Pb^{2+} in MeCN–H_2O (2 : 8; v/v) mixed medium. The fluorescence "turn on" responses enabled high fidelity nanomolar scale detection of Pb^{2+}, even over other typically competing cations like Hg^{2+} and Cd^{2+} ions. Such a "turn on" response was attributed to the consequence of CHEF. Another advantageous aspect of this study was the pronounced naked-eye colour changes (Fig. 14) of the chemosensors in the presence of Pb^{2+} (from yellow to greenish blue). Such a readily observed chromogenic colour change could prove very convenient for real-life and on-site application of the chemosensors.

The same group then developed another two pairs of chromogenic and fluorescent probes using click reactions, two of which displayed excellent selectivity and sensitivity (LOD = 2 ppb) towards Pb^{2+}.[85] Among the two Pb^{2+} chemosensors, the pyrene–triazole–carbohydrate anchored fluorophore (**42**, Scheme 11) was able to detect Pb^{2+} with the naked eye with a prominent colour change from colourless to greenish blue. The probe itself was highly fluorescent in nature, but suffered from significant quenching in the presence of Pb^{2+} in an aqueous medium (MeCN–H_2O; 2 : 8; v/v). In comparison with their previous study,[84] with replacement of the ferrocene moiety by a carbohydrate, the nature of the fluorescence response was reversed in the same semi-aqueous medium. Here, the quenching was driven by spin–orbit coupling in combination with energy transfer mechanisms. In addition, 1 : 1 binding stoichiometry and chemosensory responses of **42** towards Hg^{2+} were also documented.

Intrigued by "constitutional dynamic chemistry", Chang *et al.* adopted a new strategy to develop molecular beacon-like fluorescent probes (**43** and **44**, Scheme 11).[86] The molecular beacon-like fluorescent probes were actually two ion-pairs composed of either EDTA or sulfuric acid (the anionic counterion of the cation) and two units of residues combining an amino-containing pyrenyl derivative on a hydrophobic cholesterol backbone (cationic counterpart). EDTA and sulfuric acid were used separately as physical linkers to combine two units of the pyrene–cholesterol residues together *via* proton transfer to develop the ion-pair. Cholesterol is popular for its unique solvent polarity dependent self-assembly phenomenon and hence is regularly used as a building block of gelators of low molecular mass. The same property was observed here. Probe **43** displayed aggregation behaviour in *n*-hexane but swelling was observed in chloroform or MeOH. It was successfully utilized for the distinct recognition of two cations, Ba^{2+} and Pb^{2+}, over others tested by the development of excimer emission bands and colour changes under UV-light (Fig. 15). The probes were also successfully used to evaluate the purity of *n*-hexane, and likely the development of such biocompatible, molecular beacon-like

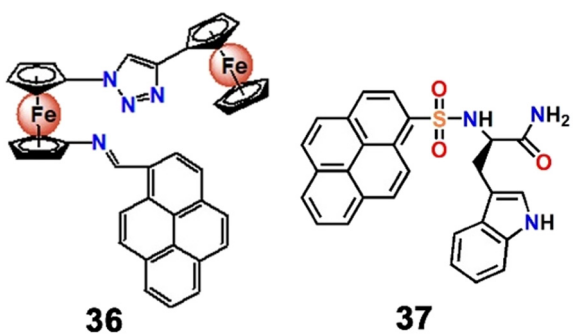

Scheme 10 Molecular structures of Pb^{2+} ion chemosensors **36** and **37**.

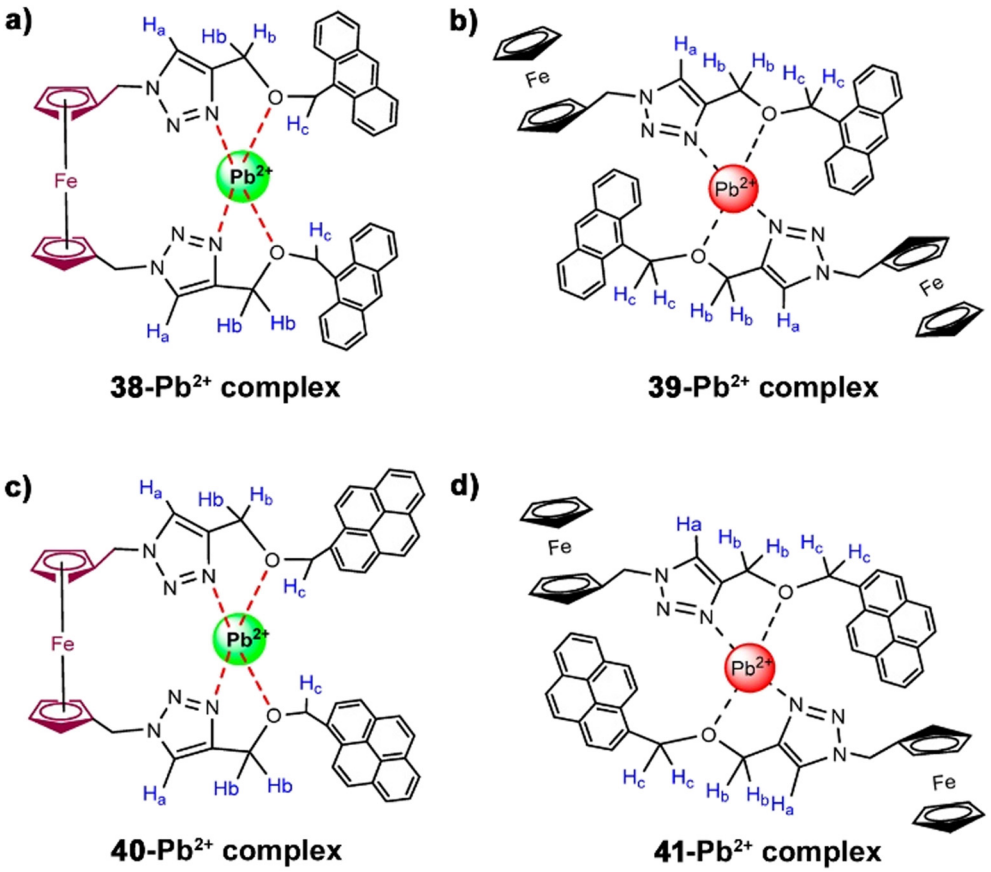

Fig. 14 Probable binding mode of (a) **38**, (b) **39**, (c) **40** and (d) **41** with Pb^{2+}; chromogenic colour change of (e) **38** and (f) **39** with different metal ions including Pb^{2+} (reproduced with permission from ref. 79. Copyright 2013, American Chemical Society).

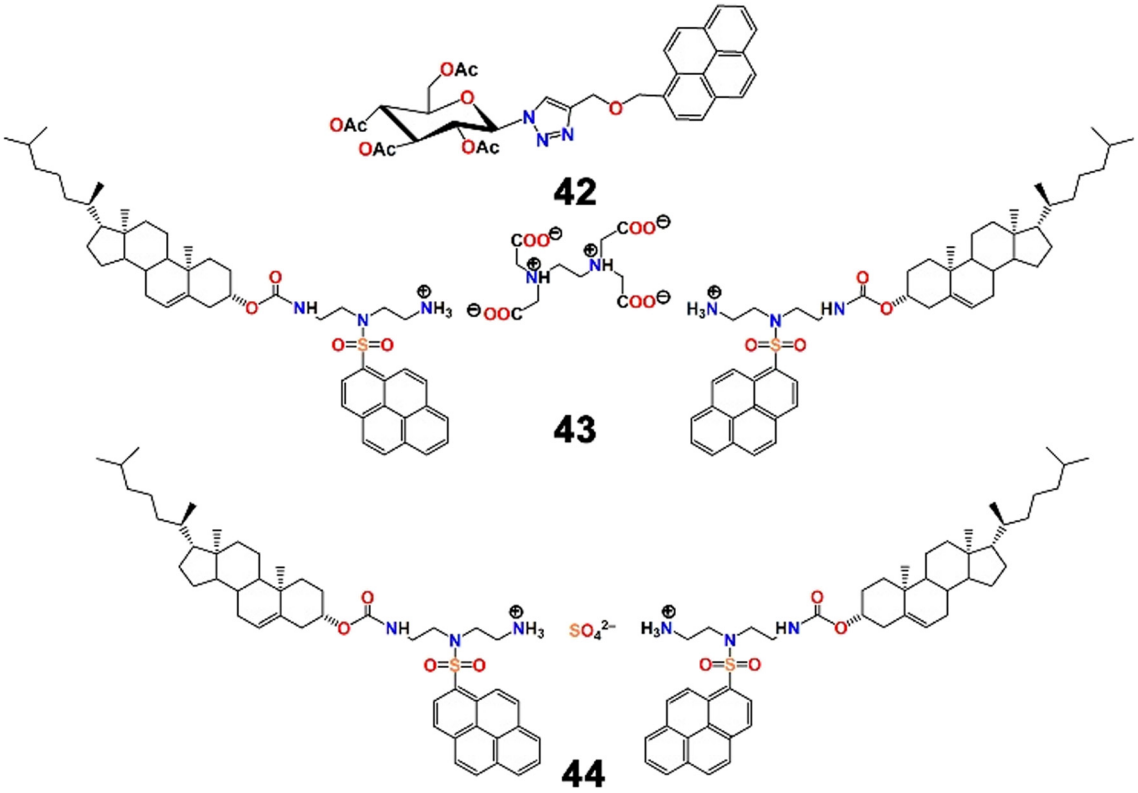

Scheme 11 Molecular structures of Pb^{2+} ion chemosensors **42**–**44**.

fluorescent sensors using this strategy is a gateway to future research in the field.

Inspired by utilising the principles of the coordination chemistry of metal ion binding and aggregation, Zhao *et al.* developed a fluorophore containing a hydrophobic group and a pair of pyrene units (fluorophore) connected by a flexible hydrophilic group (**45**, Scheme 12) and employed it for the selective and high-fidelity fluorescence detection of Fe^{3+} and Pb^{2+} ions in a semi-aqueous medium.[87] Such a molecular beacon-like shape of the probe was suitable for the formation of an excimer. As expected, in H_2O–MeCN (3 : 2; v/v) mixed solvent, the probe showed its characteristic excimer emission band at 481 nm and a poor monomeric band in the range of 370–400 nm. However, the probe displayed similar fluorescence quenching in the presence of Fe^{3+} and Pb^{2+} ions though the extent of quenching in the presence of Fe^{3+} was stronger than in the presence of Pb^{2+} (binding constant = 1.78×10^{11} and 9.60×10^{7} L^2 mol^{-2} for Fe^{3+} and Pb^{2+}, respectively). In addition, unlike Fe^{3+}, Pb^{2+} did not result in the formation of flocculent precipitates in solution. Interestingly, the fluorescence responses were almost the same over a relatively wide pH range of 4.0 to 7.5. Upon switching of the solvent to H_2O–DMSO (3 : 2; v/v), both Fe^{3+} and Pb^{2+} exhibited quenching to an almost comparable extent, with both resulting in flocculent precipitates which were white for Pb^{2+} and yellow for Fe^{3+}. The presence of a carbonyl group played a significant role in the coordination of the metal ions and the consequent development of a highly hydrophobic 1 : 1 metal complex. Remarkably, this work not only outlined the fluorescence recognition of Fe^{3+} and Pb^{2+} ions but also distinguished the two cations as well as demonstrated the removal of the metal ions from aqueous solution.

Later, Zhang *et al.* reported a new approach for the detection of multiple cations, including Pb^{2+}, in aqueous medium.[88] A composite sensor system was developed by the integration of a fluorophore, a picolyl-modified pyrene derivative (**46**, Scheme 12) and an anionic surfactant, sodium dodecyl sulfate (SDS). **46** displayed typical pyrene absorption peaks in the UV-visible range at 268, 279, 351, and 379 nm, and the emission spectra showed monomeric emission bands at 379 and 399 nm. Interestingly, the fluorophore–surfactant ensemble displayed multiple emission bands in the presence of 13 common metal ions and the fluorescent pattern was utilized in the principal component analysis (PCA) of the metal ions (Fig. 16). In addition to Pb^{2+}, the binary sensor system recognized Mg^{2+}, Al^{3+}, Ca^{2+}, Cr^{3+}, Fe^{3+}, Co^{2+}, Ni^{2+}, Cu^{2+}, Zn^{2+}, Cd^{2+}, Hg^{2+} and Ba^{2+} ions. Remarkably, this method could be employed in the discrimination of disinfected drinking water and mineral water of different brands, and the development of a binary composite sensor for the recognition and discrimination of multiple metal ions employing a PCA strategy was a remarkable innovation.

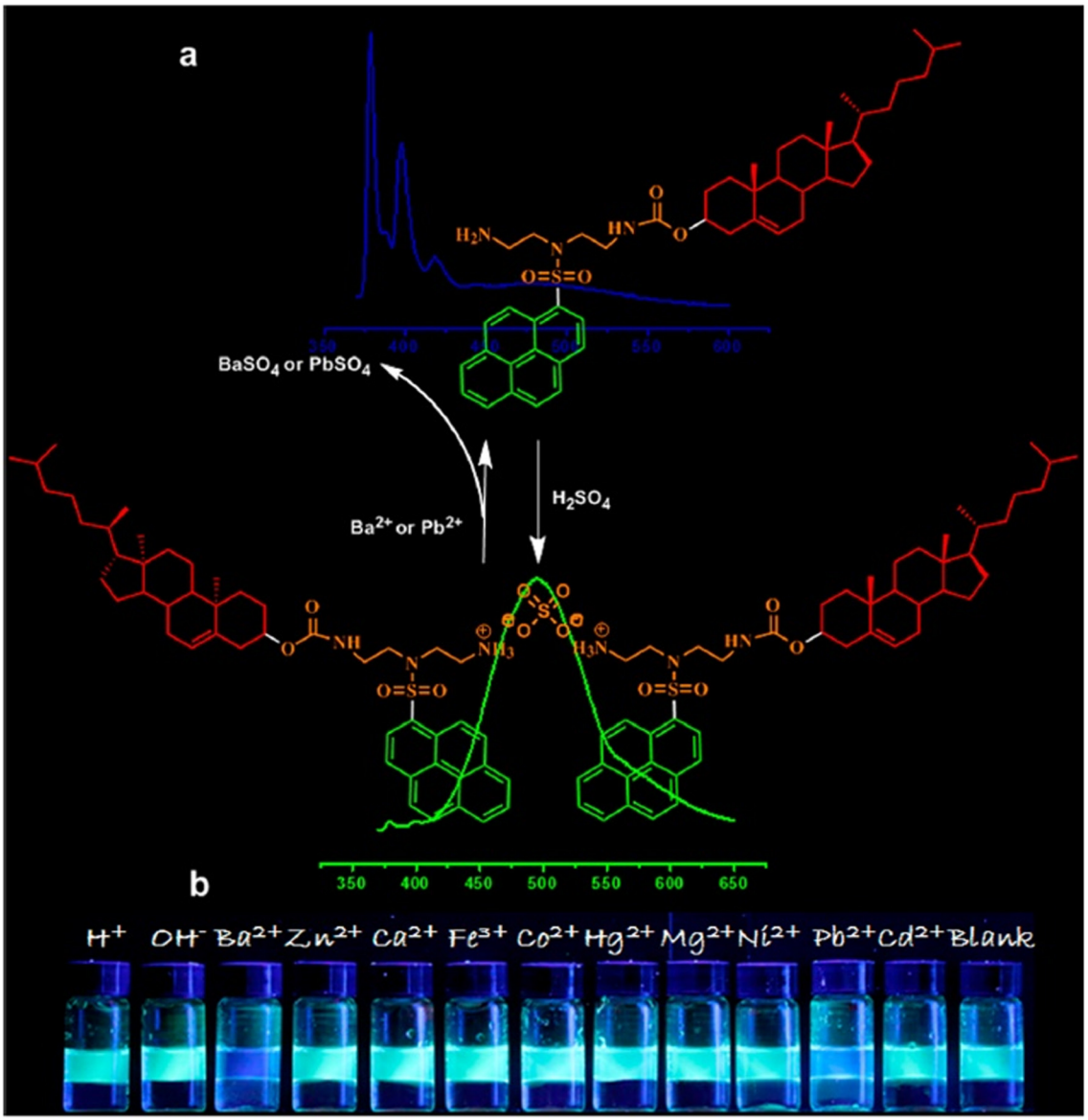

Fig. 15 Plausible binding mechanism of (a) **44** with Ba^{2+}/Pb^{2+} ions along with (b) colour change of **44** in the presence of different metal ions (reproduced with permission from ref. 86. Copyright 2015, American Chemical Society).

Recently, Merz *et al.* developed a pyrene-based "turn-off" fluorescent probe (**47**, Fig. 17) and employed it to detect and quantify environmentally important metal ions such as Cu^{2+}, Pb^{2+} and Hg^{2+}, with long fluorescence lifetimes and a rigid sensor architecture.[89] The formation of a 1:1 probe–cation complex during the course of the reaction was confirmed by Job's plot and bindfit software. In addition, at higher quencher concentrations, the Stern–Volmer plots showed a complex web of interactions that included the reversible, metal-induced production of nanosized aggregates in addition to the stoichiometric complex (Fig. 17). If the system could be immobilized on a solid base to stop aggregation, some interesting real-life application might be found.

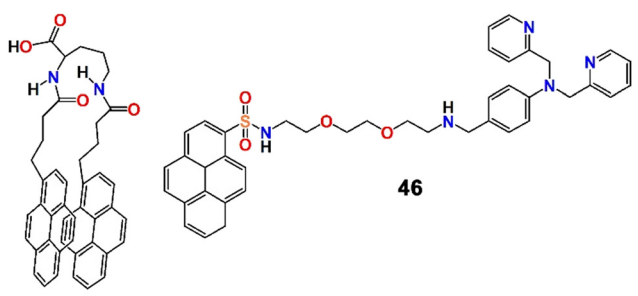

Scheme 12 Molecular structures of Pb^{2+} ion chemosensors **45** and **46**.

Here, we have observed that for the detection of Pb^{2+}, several types of binding units like calix[4]arene, triazole, indole, cholesterol, push–pull dye, pyridine, ferrocene and

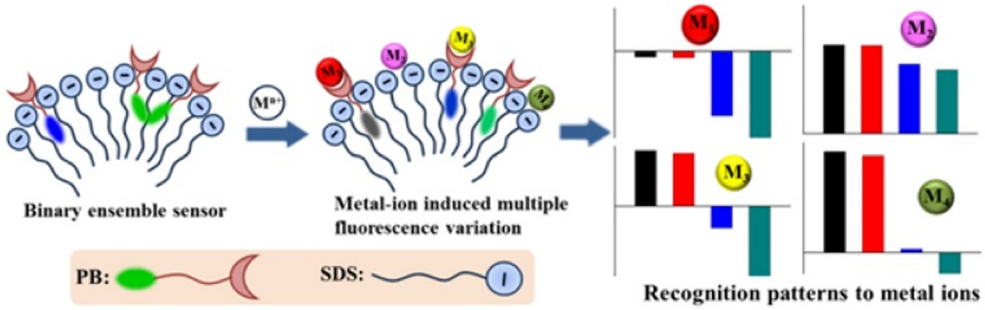

Fig. 16 Schematic diagram of the detection strategy of different metal ions by the ensemble sensor using the PCA method (reproduced with permission from ref. 88. Copyright 2017, American Chemical Society).

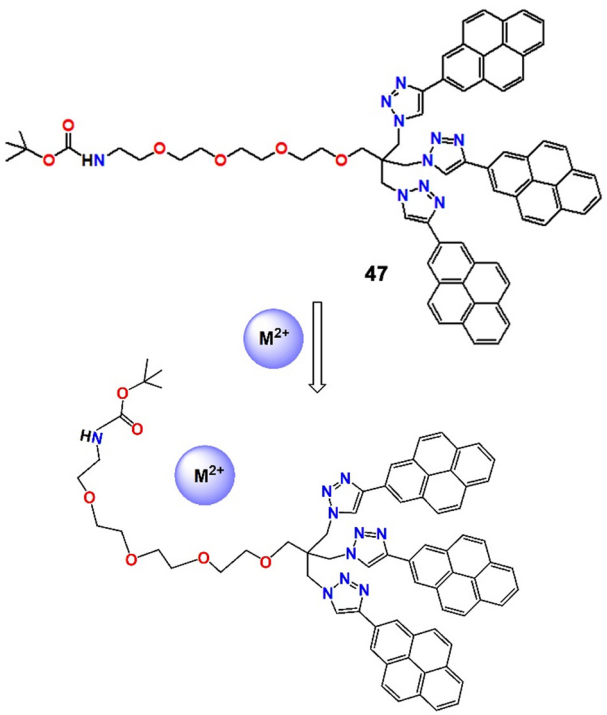

Fig. 17 Schematic diagram of the proposed binding mechanism of **47** with Cu^{2+}, Pb^{2+} and Hg^{2+} ions.

Schiff bases have been integrated with pyrenes. Also, different materials like ion-pair, molecular beacon, and fluorophore–surfactant ensemble and the PCA technique have been employed. But unlike Ag^{+} sensing, there is a huge diversity in the binding mechanism and fluorescence responses. The inclusion of Pb^{2+} into these systems has displayed a ratiometric shift of the monomer and excimer bands, quenching of either the monomer or excimer band and promotion of the excimer band. Despite all of these achievements, there is still some scope for future developments. Among all of these pyrene-based Pb^{2+} chemosensors, there are few (Table 2) that have high fidelity detection capacity in pure water. This is essential for real-life applications and is an area that needs to be developed.

As for Ag^{+}, for ease of comparison between different sensor systems, basic information like the binding unit, medium, nature of the fluorescence response, photoprocess involved, and LOD and highlights of any special features are presented.

Conclusions

This article summarizes the chronological progress on pyrene moiety-integrated small molecule chemosensors for the colorimetric and fluorescence detection of silver and lead ions. We have presented the different strategies that have been utilized for the selective recognition of lead and silver ions.

A range of different moieties have been assembled with pyrene to improve the selectivity and sensitivity of analyte detection. Most of the chemosensors reported herein displayed very sharp and distinguishable colour changes upon binding with these two metal ions and the spectroscopic responses were utilized, in the design of different high-utility and popular opto-chemical logic gates and memory units. Interestingly, in the presence of Ag^{+}, most of the pyrene-based chemosensors displayed ratiometric fluorescence changes but their application in mixed analyte samples is frequently hampered by competing responses from other analytes. In case of Pb^{2+} ion, just reversed fluorescence responses, with quenching of either the monomer or excimer emission band, were observed, rather than the more desirable ratiometric fluorescence changes being observed. Therefore, a contemporary challenge remains to establish new systems that can exploit the ratiometric potential of pyrene systems in the detection of Pb^{2+} ions. Despite the considerable number of pyrene-based chemosensors for silver and lead ions that have now been reported, none of them have yet been able to detect either of the metal ions with high fidelity in pure aqueous medium. This is an essential pre-requisite for their real-life detection and remains an enduring challenge for the future if such systems are to replace the traditional high-end analytical methods currently employed.

Table 2 Sensor information table for Pb^{2+} ion sensors containing the binding unit, medium, nature of the fluorescence response, photoprocess, LOD and any special features

Binding unit (probe number)	Medium	Fluorescence response	Photoprocess	LOD	Special feature	Ref.
Calix[4]arene (**19** and **20**)	MeCN	Quenching	PET & conformational change	—	Dual ion sensing	74
Calix[4]triazacrown (**21** and **22**)	MeCN	Quenching	PET	—	Dual ion sensing	75
Calix[4] arene-ethyleneamine-triazacrown (**23–25**)	MeCN	Quenching	PET & CHEF	—	Dual ion sensing	76
Calix[4]crown (**26** and **27**)	MeCN	Quenching	PCT & PET	—	Consecutive dual ion sensing	77
Tetrahomodioxacalix[4]arene pyreneamides (**28** and **29**)	$CHCl_3$–MeCN (1 : 3; v/v)	Quenching	PET	—	Dual ion sensing	78
Calix[4]arenes (**30–32**)	CH_2Cl_2–MeCN (1 : 1; v/v).	Quenching	PET	290 nM	Prominent naked-eye color change	79
Homooxacalix[3]arene-triazole derivative (**33** and **34**)	MeCN–H_2O–DMSO (1000 : 50 : 1; v/v)	Ratiometric	Heavy metal quenching	—	Remarkable selectivity	80
Pyridine derivative (**35**)	DMF–H_2O (1 : 1; v/v)	Quenching	Metal coordination	—	Visible light excitable fluorescent chemodosimeter	81
Ferrocene-triazole derivative (**36**)	MeCN–CH_2Cl_2 (4 : 1; v/v)	"Turn on"	CHEF	590 nM	Electrochemical and optical detection	82
Tryptophan derivative (**37**)	HEPES buffered MeCN	"Turn on"	PET	—	First report of an amino acid residue as a Pb^{2+} chemosensor	83
Triazole-tethered ferrocene (**38–41**)	MeCN–H_2O (2 : 8; v/v)	"Turn on"	CHEF	2 ppb	Sharp naked-eye color change	84
Triazole-carbohydrate derivative (**42**)	MeCN–H_2O (2 : 8; v/v)	Quenching	Spin–orbit coupling & energy transfer	2.0 nM	Sharp naked-eye color change	85
Cholesterol amino acid anchored molecular beacon (**43** and **44**)	$CHCl_3$–*n*-hexane	Quenching	Monomer–excimer conversion	—	Ion-pair as a chemosensor	86
Butyroyl-ornithine derivative (**45**)	H_2O–DMSO (3 : 2; v/v)	Quenching	Aggregation	—	Solvent-dependent ion sensing behavior	87
Bis(2-picolyl)amine-modified pyrene-SDS composite (**46**)	H_2O	—	Aggregation	—	Application of the PCA method	88
Tetraethylene glycol-triazole derivative (**47**)	MeCN	Quenching	Aggregation	600 nM	Multiple metal ion sensing	89

Abbreviations

CHEF	Chelation enhanced fluorescence
DFT	Density functional theory
EDTA	Ethelene diamine tetraacetic acid
HB	Hydrogen bonding
ICT	Intramolecular charge transfer
LOD	Limit of detection
MB	Molecular beacon
PA	Picric acid
PCA	Principal component analysis
PCT	Photoinduced charge transfer
PET	Photoinduced electron transfer
SDS	Sodium dodecyl sulfate

Conflicts of interest

There are no conflicts to declare.

Acknowledgements

SP and ND acknowledge the Central Analytical Laboratory, Department of Chemistry, BITS-Pilani, Hyderabad Campus, India. PB acknowledges the Department of Chemistry, Kaliyaganj College for support. PB also acknowledges the financial support from the Science and Engineering Research Board (SERB), India (SRG/2022/001562).

Notes and references

1 D. Wu, A. C. Sedgwick, T. Gunnlaugsson, E. U. Akkaya, J. Yoon and T. D. James, Fluorescent chemosensors: The past, present and future, *Chem. Soc. Rev.*, 2017, **46**, 7105–7123.
2 M. Vendrell, D. Zhai, J. C. Er and Y.-T. Chang, Combinatorial strategies in fluorescent probe development, *Chem. Rev.*, 2012, **112**, 4391–4420.
3 S. Paul, T. Majumdar and A. Mallick, Hydrogen bond regulated hydrogen sulfate ion recognition: an overview, *Dalton Trans.*, 2021, **50**, 1531–1549.
4 S. Paul, P. Paul, S. Samanta, T. Majumdar and A. Mallick, Hydrogen bond directed high-fidelity optical detection of picric acid: A single driver on diverse roads towards the same destiny, *Org. Biomol. Chem.*, 2023, **21**, 3503–3524.
5 S. Paul, P. Daga and N. Dey, Exploring various photochemical processes in optical sensing of pesticides by luminescent nanomaterials: A concise discussion on challenges and recent advancements, *ACS Omega*, 2023, **8**, 44395–44423.

6 S. Paul, M. Karar and N. Dey, Sequence specific optical recognition of dual Anions, fluoride and bisulfate ions: An update, *J. Mol. Liq.*, 2024, **394**, 123524.
7 K. Ayyavoo and P. Velusamy, Pyrene-based materials as fluorescent probes in chemical and biological fields, *New J. Chem.*, 2021, **45**, 10997–11017.
8 Z. Kowser, U. Rayhan, T. Akther, C. Redshaw and T. Yamato, A brief review on novel pyrene based fluorimetric and colorimetric chemosensors for the detection of Cu^{2+}, *Mater. Chem. Front.*, 2021, **5**, 2173–2200.
9 S. Saha, S. Paul, R. Debnath, N. Dey and B. Biswas, AIE active fluorescent organic nanoparticles based optical detection of Cu^{2+} ions in pure water: a case of aggregation-disaggregation reversibility, *Anal. Methods*, 2024, **16**, 1058–1068.
10 M. Qiao, J. Fan, L. Ding and Y. Fang, Fluorescent ensemble sensors and arrays based on surfactant aggregates encapsulating pyrene-derived fluorophores for differentiation applications, *ACS Appl. Mater. Interfaces*, 2021, **13**, 18395–18412.
11 M. Shellaiah and K.-W. Sun, Pyrene-based AIE active materials for bioimaging and theranostics applications, *Biosensors*, 2022, **12**, 550.
12 T. M. Figueira-Duarte and K. Mullen, Pyrene-based materials for organic electronics, *Chem. Rev.*, 2011, **111**, 7260–7314.
13 M. M. Islam, Z. Hu, Q. Wang, C. Redshaw and X. Feng, Pyrene-based aggregation-induced emission luminogens and their applications, *Mater. Chem. Front.*, 2019, **3**, 762–781.
14 K. Kalyanasundaram and J. K. Thomas, Environmental effects on vibronic band intensities in pyrene monomer fluorescence and their application in studies of micellar systems, *J. Am. Chem. Soc.*, 1977, **99**, 2039–2044.
15 J. B. Birks, *Photophysics of aromatic molecules*, Wiley-Interscience, New York, NY, 1970, p. 301.
16 J. B. Birks, M. D. Lumb, I. H. Munro and B. H. Flowers, 'Excimer' fluorescence V. Influence of solvent viscosity and temperature, *Proc. R. Soc. London, Ser. A*, 1964, **280**, 289–297.
17 P. C. Johnson and H. W. Offen, Effect of pressure on pyrene excimer fluorescence in toluene, *J. Chem. Phys.*, 1972, **56**, 1638–1642.
18 M. R. Pokhrel and S. H. Bossmann, Synthesis, characterization, and first application of high molecular weight polyacrylic acid derivatives possessing perfluorinated side chains and chemically linked pyrene labels, *J. Phys. Chem. B*, 2000, **104**, 2215–2223.
19 X. Feng, X. Wang, C. Redshaw and B. Z. Tang, Aggregation behaviour of pyrene-based luminescent materials, from molecular design and optical properties to application, *Chem. Soc. Rev.*, 2023, **52**, 6715–6753.
20 D. T. Quang and J. S. Kim, Fluoro- and chromogenic chemodosimeters for heavy metal ion detection in solution and biospecimens, *Chem. Rev.*, 2010, **110**, 6280–6301.
21 K. P. Carter, A. M. Young and A. E. Palmer, Fluorescent sensors for measuring metal ions in living systems, *Chem. Rev.*, 2014, **114**, 4564–4601.
22 S. Baar, The effect of silver compounds on the metabolism of human red cells, *Burns*, 1975, **2**, 58–66.
23 H. Wang, N. Law, G. Pearson, B. E. van Dongen, R. M. Jarvis, R. Goodacre and J. R. Lloyd, Impact of silver(I) on the metabolism of shewanella oneidensis, *J. Bacteriol.*, 2010, **192**, 1143–1150.
24 E. S. Claudio, H. A. Godwin and J. S. Magyar, Fundamental coordination chemistry, environmental chemistry, and biochemistry of Lead(II), *Prog. Inorg. Chem.*, ed. K. D. Karlin, 2003, ch. I, vol. 51, pp. 1–144.
25 M. S. Collin, S. K. Venkatraman, N. Vijayakumar, V. Kanimozhi, S. M. Arbaaz, R. G. S. Stacey, J. Anusha, R. Choudhary, V. Lvov, G. I. Tovar, F. Senatov, S. Koppala and S. Swamiappan, Bioaccumulation of lead (Pb) and its effects on human: A review, *J. Hazard. Mater. Adv.*, 2022, **7**, 100094.
26 S. Singha, D. Kim, H. Seo, S. W. Cho and K. H. Ahn, Fluorescence sensing systems for gold and silver species, *Chem. Soc. Rev.*, 2015, **44**, 4367–4399.
27 J. F. Zhang, Y. Zhou, J. Yoon and J. S. Kim, Recent progress in fluorescent and colorimetric chemosensors for detection of precious metal ions (silver, gold and platinum ions), *Chem. Soc. Rev.*, 2011, **40**, 3416–3429.
28 M. Yamanaka, K. Hara and J. Kudo, Bactericidal actions of a silver ion solution on Escherichia coli, studied by energy-filtering transmission electron microscopy and proteomic analysis, *Appl. Environ. Microbiol.*, 2005, **71**, 7589–7593.
29 J. A. Lemire, J. J. Harrison and R. J. Turner, Antimicrobial activity of metals: mechanisms, molecular targets and applications, *Nat. Rev. Microbiol.*, 2013, **11**, 371–384.
30 L. P. Padhye, T. Jasemizad, S. Bolan, O. V. Tsyusko, J. M. Unrine, B. K. Biswal, R. Balasubramanian, Y. Zhang, T. Zhang, J. Zhao, Y. Li, J. Rinklebe, H. Wang, K. H. M. Siddique and N. Bolan, Silver contamination and its toxicity and risk management in terrestrial and aquatic ecosystems, *Sci. Total Environ.*, 2023, **871**, 161926.
31 C. M. Litwin, S. A. Boyko and S. B. Calderwood, Cloning, sequencing, and transcriptional regulation of the Vibrio cholerae for gene, *J. Bacteriol.*, 1992, **174**, 1897–1903.
32 M. R. Ganjali, P. Norouzi, T. Alizadeh and M. Adib, Ion recognition: synthesis of 2-methyl-2, 4-di(2-thienyl)-2,3-dihydro-1H-1,5-benzodiazepine and its application in construction of a highly selective and sensitive Ag+ membrane sensors, *J. Braz. Chem. Soc.*, 2006, **17**, 1217–1222.
33 H. N. Kim, W. X. Ren, J. S. Kim and J. Yoon, Fluorescent and colorimetric sensors for detection of lead, cadmium, and mercury ions, *Chem. Soc. Rev.*, 2012, **41**, 3210–3244.
34 World Health Organization, *Guidelines for drinking-water quality*, Geneva, 3rd edn, 2004, vol. 1, p. 188.
35 A. R. Flegal and D. R. Smith, Current needs for increased accuracy and precision in measurements of low levels of lead in blood, *Environ. Res.*, 1992, **58**, 125–133.
36 Departments of Health and Human Services and Prevention, Center for disease control (2003) surveillance for elevated blood lead levels among childrens: United States, 1997–2001, *Morbidity and Mortality Weekly Rep.*, 52, p. 1.
37 D. Wu, Y. Hu, H. Cheng and X. Ye, Detection techniques for lead ions in water: A review, *Molecules*, 2023, **28**, 3601.

38 B. Alies, M. A. Ouelhazi, A. Noireau, K. Gaudin and P. Barthelemy, Silver ions detection *via* nucleolipids self-assembly, *Anal. Chem.*, 2019, **91**, 1692–1695.
39 J. Wu, J. Yu, J. Li, J. Wang and Y. Ying, Detection of metal ions by atomic emission spectroscopy from liquid-electrode discharge plasma, *Spectrochim. Acta, Part B*, 2007, **62**, 1269–1272.
40 A. A. Ammann, Speciation of heavy metals in environmental water by ion chromatography coupled to ICP-MS, *Anal. Bioanal. Chem.*, 2002, **372**, 448–452.
41 R. Silva, K. Zhao, R. Ding, W. P. Chan, M. Yang, J. S. Q. Yip and G. Lisak, *Analyst*, 2022, **147**, 4500–4509.
42 L. A. Hutton, G. D. O'Neil, T. L. Read, Z. J. Ayres, M. E. Newton and J. V. Macpherson, Electrochemical x-ray fluorescence spectroscopy for trace heavy metal analysis: Enhancing x-ray fluorescence detection capabilities by four orders of magnitude, *Anal. Chem.*, 2014, **86**, 4566–4572.
43 A. Mourya, B. Mazumdar and S. K. Sinha, Determination and quantification of heavy metal ion by electrochemical method, *J. Environ. Chem. Eng.*, 2019, **7**, 103459.
44 A. Waheed, M. Mansha and N. Ullah, Nanomaterials-based electrochemical detection of heavy metals in water: Current status, challenges and future direction, *TrAC, Trends Anal. Chem.*, 2018, **105**, 37–51.
45 M. Jin, H. Yuan, B. Liu, J. Peng, L. Xu and D. Yang, Review of the distribution and detection methods of heavy metals in the environment, *Anal. Methods*, 2020, **12**, 5747–5766.
46 Y. Zhou, Z. Xu and J. Yoon, Fluorescent and colorimetric chemosensors for detection of nucleotides, FAD and NADH: highlighted research during 2004-2010, *Chem. Soc. Rev.*, 2011, **40**, 2222–2235.
47 Y. Lin, D. Gritsenko, S. Feng, Y. C. Teh, X. Lu and J. Xu, Detection of heavy metal by paper-based microfluidics, *Biosens. Bioelectron.*, 2016, **83**, 256–266.
48 S. Li, C. Zhang, S. Wang, Q. Liu, H. Feng, X. Ma and J. Guo, Electrochemical microfluidics techniques for heavy metal ion detection, *Analyst*, 2018, **143**, 4230–4246.
49 G. Aragay, J. Pons and A. Merkoçi, Recent trends in macro-, micro-, and nanomaterial-based tools and strategies for heavy-metal detection, *Chem. Rev.*, 2011, **111**(5), 3433–3458.
50 H. Singh, A. Bamrah, S. K. Bhardwaj, A. Deep, M. Khatri, R. J. C. Brown, N. Bhardwaj and K.-H. Kim, Recent advances in the application of noble metal nanoparticles in colorimetric sensors for lead ions, *Environ. Sci.: Nano*, 2021, **8**, 863–889.
51 I. Stassen, N. Burtch, A. Talin, P. Falcaro, M. Allendorf and R. Ameloot, An updated roadmap for the integration of metal-organic frameworks with electronic devices and chemical sensors, *Chem. Soc. Rev.*, 2017, **46**, 3185–3241.
52 M. Li, Q. Shi, N. Song, Y. Xiao, L. Wang, Z. Chen and T. D. James, Current trends in the detection and removal of heavy metal ions using functional materials, *Chem. Soc. Rev.*, 2023, **52**, 5827–5860.
53 N. Dey, Naked-eye sensing of phytic acid at sub-nanomolar levels in 100% water medium by a charge transfer complex derived from off-the-shelf ingredients, *Analyst*, 2020, **145**, 4937–4941.
54 N. Dey, A pyrene-based ratiometric probe for nanomolar level detection of glyphosate in food and environmental samples and its application for live-cell imaging, *New J. Chem.*, 2022, **46**, 8105–8111.
55 N. Dey and N. Kumari, Anion-induced deprotonation as a simple strategy to improve analytical performance of an amphiphilic probe at mesoscopic interface, *Results Chem.*, 2022, **4**, 100248.
56 S. Paul, A. R. Choudhury and N. Dey, Dual-mode multiple ion sensing *via* analyte-specific modulation of keto-enol tautomerization of an ESIPT active pyrene derivative: Experimental findings and computational rationalization, *ACS Omega*, 2023, **8**, 6349–6360.
57 S. Paul, S. Mondal and N. Dey, Improved analytical performance of an amphiphilic probe upon protein encapsulation: Spectroscopic investigation along with computational rationalization, *ACS Appl. Bio Mater.*, 2023, **6**, 1495–1503.
58 R. S. Fernandes and N. Dey, A combinatorial effect of TICT and AIE on bisulfate detection using a pyrenylated charge-transfer Luminogen, *Mater. Res. Bull.*, 2023, **163**, 112192.
59 S. Mondal, M. Karar and N. Dey, Dye-surfactant co-assembly as the chromogenic indicator for nanomolar level detection of Cu(I) ions *via* a color-changing response, *J. Mater. Chem. B*, 2023, **11**, 4111–4120.
60 S. Kim, O. J. Shon, J. A. Rim, S. K. Kim and J. Yoon, Pyrene-armed calix[4]azacrowns as new fluorescent ionophores: "Molecular Taekowndo" process *via* fluorescence change, *J. Org. Chem.*, 2002, **67**, 2348–2351.
61 S.-H. Park, N. Kwon, J.-H. Lee, J. Yoon and I. Shin, Synthetic ratiometric fluorescent probes for detection of ions, *Chem. Soc. Rev.*, 2020, **49**, 143–179.
62 A. Bigdeli, F. Ghasemi, S. Abbasi-Moayed, M. Shahrajabian, N. Fahimi-Kashani, S. Jafarinejad, M. A. F. Nejad and M. R. Hormozi-Nezhad, Ratiometric fluorescent nanoprobes for visual detection: Design principles and recent advances - A review, *Anal. Chim. Acta*, 2019, **1079**, 30–58.
63 R.-H. Yang, W.-H. Chan, A. W. M. Lee, P.-F. Xia, H.-K. Zhang and K. A. Li, A ratiometric fluorescent sensor for Ag^{I} with high selectivity and sensitivity, *J. Am. Chem. Soc.*, 2003, **125**, 2884–2885.
64 M. Kumar, R. Kumar and V. Bhalla, Optical chemosensor for Ag^{+}, Fe^{3+}, and cysteine: Information processing at molecular level, *Org. Lett.*, 2011, **13**, 366–369.
65 F. Wang, R. Nandhakumar, J. H. Moon, K. M. Kim, J. Y. Lee and J. Yoon, Ratiometric fluorescent chemosensor for silver ion at physiological pH, *Inorg. Chem.*, 2011, **50**, 2240–2245.
66 S. Jang, P. Thirupathi, L. N. Neupane, J. Seong, H. Lee, W. I. Lee and K.-H. Lee, Highly sensitive ratiometric fluorescent chemosensor for silver ion and silver nanoparticles in aqueous solution, *Org. Lett.*, 2012, **14**, 4746–4749.
67 N.-J. Wang, C.-M. Sun and W.-S. Chung, A highly selective fluorescent chemosensor for Ag^{+} based on calix[4]arene with

lower-rim proximal triazolylpyrenes, *Sens. Actuators, B*, 2012, **171–172**, 984–993.
68 J. Fernández-Lodeiro, C. Núñez, C. S. de Castro, E. Bértolo, J. S. S. de Melo, J. L. Capelo and C. Lodeiro, Steady-state and time-resolved investigations on pyrene-based chemosensors, *Inorg. Chem.*, 2013, **52**, 121–129.
69 K. Velmurugan, A. Raman, S. Easwaramoorthi and R. Nandhakumar, Pyrene pyridine-conjugate as Ag selective fluorescent chemosensor, *RSC Adv.*, 2014, **4**, 35284–35289.
70 X. Chang, Z. Wang, Y. Qi, R. Kang, X. Cui, C. Shang, K. Liu and Y. Fang, Dynamic chemistry-based sensing: A molecular system for detection of saccharide, formaldehyde, and the silver ion, *Anal. Chem.*, 2017, **89**, 9360–9367.
71 W. Zhang, Y. Luo, Y. Zhou, M. Liu, W. Xu, B. Bian, Z. Tao and X. Xiao, A highly selective fluorescent chemosensor probe for detection of Fe^{3+} and Ag^{+} based on supramolecular assembly of cucurbit[10]uril with a pyrene derivative, *Dyes Pigm.*, 2020, **176**, 108235–110841.
72 J. Rodríguez-Lavado, A. Lorente, E. Flores, A. Ochoa, F. Godoy, P. Jaque and C. Saitz, Elucidating sensing mechanisms of a pyrene excimer-based calix[4]arene for ratiometric detection of Hg(II) and Ag(I) and chemosensor behaviour as INHIBITION or IMPLICATION logic gates, *RSC Adv.*, 2020, **10**, 21963–21973.
73 H. Ju, A. Taniguchi, K. Kikukawa, H. Horita, M. Ikeda, S. Kuwahara and Y. Habata, Argentivorous molecules with chromophores in side arms: Silver ion-induced turn on and turn off of fluorescence, *Inorg. Chem.*, 2021, **60**, 9141–9147.
74 S. K. Kim, S. H. Lee, J. Y. Lee, J. Y. Lee, R. A. Bartsch and J. S. Kim, An excimer-based, binuclear, on-off switchable calix[4]crown chemosensor, *J. Am. Chem. Soc.*, 2004, **126**, 16499–16506.
75 J. Y. Lee, S. K. Kim, J. H. Jung and J. S. Kim, Bifunctional fluorescent calix[4]arene chemosensor for both a cation and an anion, *J. Org. Chem.*, 2005, **70**, 1463–1466.
76 S. H. Lee, S. H. Kim, S. K. Kim, J. H. Jung and J. S. Kim, Fluorescence ratiometry of monomer/excimer emissions in a space-through PET system, *J. Org. Chem.*, 2005, **70**, 9288–9295.
77 J. K. Choi, S. H. Kim, J. Yoon, K.-H. Lee, R. A. Bartsch and J. S. Kim, A PCT-based, pyrene-armed calix[4]crown fluoroionophore, *J. Org. Chem.*, 2006, **71**, 8011–8015.
78 J. K. Choi, A. Lee, S. Kim, S. Ham, K. No and J. S. Kim, Fluorescent ratiometry of tetrahomodioxacalix[4]arene pyrenylamides upon cation complexation, *Org. Lett.*, 2006, **8**, 1601–1604.
79 M. Kumar, J. N. Babu, V. Bhalla and R. Kumar, Ratiometric/'On–Off' sensing of Pb^{2+} ion using pyrene-appended calix[4]arenes, *Sens. Actuators, B*, 2010, **144**, 183–191.
80 X.-L. Ni, S. Wang, X. Zeng, Z. Tao and T. Yamato, Pyrene-linked triazole-modified homooxacalix[3]arene: A unique C_3 symmetry ratiometric fluorescent chemosensor for Pb^{2+}, *Org. Lett.*, 2010, **13**, 552–555.
81 L. Wang, M. Yu, Z. Liu, W. Zhao, Z. Li, Z. Ni, C. Li and L. Wei, A visible light excitable "on-off" and "green-red" fluorescent chemodosimeter for Ni^{2+}/Pb^{2+}, *New J. Chem.*, 2012, **36**, 2176–2179.
82 F. Oton, M. del C. Gonzalez, A. Espinosa, A. Tarraga and P. Molina, Synthesis, structural characterization, and sensing properties of clickable unsymmetrical 1,1′-disubstituted ferrocene-triazole derivatives, *Organometallics*, 2012, **31**, 2085–2096.
83 L. N. Neupane, J.-Y. Park, J. H. Park and K.-H. Lee, Turn-on fluorescent chemosensor based on an amino acid for Pb(II) and Hg(II) ions in aqueous solutions and role of tryptophan for sensing, *Org. Lett.*, 2013, **15**, 254–257.
84 A. Thakur, D. Mandal and S. Ghosh, Sensitive and selective redox, chromogenic, and "Turn-On" fluorescent probe for Pb(II) in aqueous environment, *Anal. Chem.*, 2013, **85**, 1665–1674.
85 A. Thakur, D. Mandal, P. Deb, B. Mondal and S. Ghosh, Synthesis of triazole linked fluorescent amino acid and carbohydrate bio-conjugates: A highly sensitive and skeleton selective multi-responsive chemosensor for Cu(II) and Pb(II)/Hg(II) ions, *RSC Adv.*, 2014, **4**, 1918–1928.
86 X. Chang, C. Yu, G. Wang, J. Fan, J. Zhang, Y. Qi, K. Liu and Y. Fang, Constitutional dynamic chemistry-based new concept of molecular beacons for high efficient development of fluorescent probes, *J. Phys. Chem. B*, 2015, **119**, 6721–6729.
87 M. Zhao, X. Zhou, J. Tang, Z. Deng, X. Xu, Z. Chen, X. Li, L. Yang and L.-J. Ma, Pyrene excimer-based fluorescent sensor for detection and removal of Fe^{3+} and Pb^{2+} from aqueous solutions, *Spectrochim. Acta, Part A*, 2017, **173**, 235–240.
88 L. Zhang, X. Huang, Y. Cao, Y. Xin and L. Ding, Fluorescent binary ensemble based on pyrene derivative and sodium dodecyl sulfate assemblies as a chemical tongue for discriminating metal ions and brand water, *ACS Sens.*, 2017, **2**, 1821–1830.
89 V. Merz, J. Merz, M. Kirchner, J. Lenhart, T. B. Marder and A. Krueger, Pyrene-based "Turn-Off" probe with broad detection range for Cu^{2+}, Pb^{2+} and Hg^{2+} ions, *Chem. – Eur. J.*, 2021, **27**, 8118–8126.